




Probabilistic Seismic Hazard Assessment of Mangalore and Its Adjoining Regions, A Part of Indian Peninsular: An Intraplate Region

C. SHREYASVI,¹  KATTA VENKATARAMANA,¹ SUMER CHOPRA,² and MADAN MOHAN ROUT²

Abstract—The Southwestern part of India investigated in the present study mainly comprises of states such as Goa, north Kerala and a major portion of Karnataka. A comprehensive regional seismic catalog has been compiled spanning over 190 years apart from a few prehistoric events from the early 16th century. The classical Cornell–McGuire approach has been incorporated in the estimation of seismic hazard. The seismic sources are modeled as area sources and the entire study region is divided into four seismogenic source zones. The uncertainties involved in the formulation of the seismic source model and ground motion prediction model has been discussed in detail. Further, the procedure for selecting appropriate GMPEs involves the evaluation of multidimensional (M, R, T) ground motion trends and performance against observed macroseismic data. The epistemic uncertainty in the estimation of seismicity parameters and ground motion prediction equations (GMPEs) has been addressed using logic tree computation. The results of the hazard analysis demonstrate that the existing seismic code underestimates the seismic potential of seismic zone II (BIS 1893) areas. The de-aggregation of the predicted seismic hazard revealed earthquakes of magnitude range (M_w) 4–6 occurring within a distance of 35kms to be most influential for any given site of interest. Sensitivity analysis has been performed for crucial input parameters in the formulation of seismic source and ground motion models. Site amplification study has been carried out using topographic slope as a proxy to shear velocity in the top 30 m (V_{s30}). A maximum of 60% to 80% amplification has been observed in the study area. The seismic hazard maps in terms of PGA have been plotted for the seismic hazard estimated at the bedrock level as well as the surface level for 2% and 10% probability of exceedance in 50 years. The hazard estimation specifically for the southern part of the west coast is the first of its kind. The investigation suspects mining-induced seismicity in Bellary and Raichur districts though there is no mention of this in the prior literature.

Key words: Regional earthquake catalog, seismicity parameters, Trellis plots, de-aggregation of seismic hazard, surface topography, hazard maps.

1. Introduction

Earthquakes are known to have an enormous impact on human life. The unpredictable nature of the earthquakes has provoked interest among researchers for a few decades now and continue to challenge mankind in finding a sustainable solution. The earlier records of historical earthquakes reveal about seismic activity in Dholavira (Khadir islet of Kachchh, India) in the year 2200 BC supported by the evidence of ground displacement and the collapse of walls. Most widely accepted explanation for seismic activity in Indian peninsula is the ongoing subduction of the Indian plate under the Eurasian plate resulting in sporadic seismic activity in Southern India. The earthquakes observed in this region are of intraplate nature and mostly shallow focussed causing extensive damage to life and building stock. The Bhuj earthquake (2001) shattered the ‘seismically stable’ status of Peninsular India and demonstrated the necessity for earthquake studies in this region.

Mangalore is one of the coastal cities located on the West coast of India in Karnataka (one of the states in India) and a major commercial hub for the state. The city is alongside the Arabian Sea on the west and the Western Ghats on the east making its topography vary from plain on the coastal side to undulating hilly terrain towards its east. The city houses a whole bunch of petrochemical industries apart from being India’s eighth largest port and the fourth-largest city in the state in terms of population. In addition, the Bureau of Indian Standards (IS 1893, 2016) has identified Mangalore and its surrounding area as a moderately earthquake-prone urban center, categorizing it under seismic zone III. This zone can be characterized as moderate damage risk zone liable to

¹ Department of Civil Engineering, National Institute of Technology Karnataka, Surathkal, Srinivasnagar Post, Mangalore, Karnataka 575025, India. E-mail: shreyasvic@gmail.com

² Institute of Seismological Research, Raisan, Gandhinagar, Gujarat 382009, India.

an intensity of VII on the MSK scale with a zone factor of 0.16 g (PGA). Further, the study area includes dams such as Supa, Krishnaraja Sagara, Linganamakki and many other along with few mining areas such as Kudremukh, Raichur, and Bellary. Owing to its socio-economic importance, the task of characterizing and evaluating the hazard potential in making the urban and rural sectors resilient towards seismic activity is inordinately vital.

In order to achieve the same, it is necessary to quantify the severity of ground shaking that can be expected in the region which involves a great deal of uncertainty in location, size and resulting intensity of forthcoming earthquakes. Probabilistic seismic hazard analysis (PSHA) aims to quantify these uncertainties and present a reasonable estimate of the exceedance probability of a certain intensity measure (PGA, PSA, S_a at 5% damping) in a given time frame. The methodology estimated the hazard level for various return periods by exploring all the possible combinations of magnitude and distances of seismic activity with due consideration to local site effects. In this study, the existing seismotectonic features in Mangalore and its surrounding region coupled with the past earthquake statistics is used in understanding the seismic potential of the study area that is further made use of in making a plausible assessment of the seismic hazard.

The analytical framework for evaluating the seismic hazard in a probabilistic manner was first introduced by Cornell (1968). In recent years, many researchers have focused on quantifying the seismic hazard for the whole of peninsular India as well as for smaller regions taken as independent studies. The probabilistic seismic hazard map for India and the adjoining regions was generated by Khattri et al. (1984) by dividing the entire study region into 24 seismic zones and adopting distance attenuation laws developed for Eastern North America. A similar work was carried out by Bhatia et al. (1999) for the same region under Global Seismic Hazard Assessment Program (GSHAP) and peak ground acceleration was determined at the center of each grid of size $0.5^\circ \times 0.5^\circ$. Peninsular India was considered to be a stable continental landmass until it was hit by few major intraplate earthquakes such as Latur (M_w : 6.2, 1993), Jabalpur (M_w : 5.8, 1997) and Bhuj (M_w : 7.7,

2001) in recent times. These events inspired further research into understanding the seismotectonics of intraplate regions. Jaiswal and Sinha (2007) combined observed seismicity and known geological characteristics in identifying 9 seismogenic source zones in peninsular India. Additionally, they adopted a zone free method to estimate the seismic hazard. Ashish et al. (2016) distinguished Gujarat region from the rest of peninsular India by characterizing it as an active crustal region and adopted multiple seismicity models in estimating the seismic hazard. Apart from the studies carried out for the entire Indian subcontinent, hazard quantification has been performed for important cities such as Delhi (Iyengar and Ghosh 2004), Bangalore (Anbazhagan et al. 2009), Gujarat (Chopra et al. 2013), Mumbai (Desai and Choudhury 2014), North East India (Das et al. 2016), West Bengal (Maiti et al. 2017), Himalayan region (Rout et al. 2018).

The seismic hazard can be estimated for various soil conditions as well as at the bedrock level. The generated hazard curve at the bedrock level can be further used in generating a site-specific Uniform Hazard Spectrum (UHS) by modeling the local site conditions. In the absence of sufficient, site-specific data, a more generic method can be used to assess the overall amplification potential of a wider study region. The amplification or attenuation of the seismic waves traveling from bedrock to surface depends on the characteristics of the soil constituting the medium for propagation. Shear wave velocity in the top 30 m ($V_{s(30)}$) is the most widely chosen parameter for assessing the dynamic characteristics of the soil. In addition to the in situ techniques available for measuring $V_{s(30)}$, Allen and Wald (2009) provided an indirect measure by correlating it to topography.

The present study is an attempt to understand the seismic potential of Mangalore and its surrounding region. This has been realized by considering the past earthquake activity witnessed in the region along with the available information on seismotectonic features. The past earthquake data was collected from various global and local sources and processed further to obtain seismicity parameters. The entire study region has been divided into four seismogenic source zones and the seismicity parameters are estimated for each of these zones by maximum likelihood approach.

Regionally applicable ground motion prediction equations (GMPEs) were investigated qualitatively and four GMPEs were chosen for estimating the ground motion. The estimated hazard has been presented in the form of hazard curve and Uniform Hazard Spectrum (UHS) for a reference site condition (NEHRP A, $V_s > 1500 \text{ ms}^{-1}$). The shear velocity profile for the entire study region has been developed using the Digital Elevation Model (DEM) data. The modification in the ground motion parameter from the bedrock at a depth to surface level has been captured using the amplification equation suggested by Raghu Kanth and Iyengar (2007). The predicted seismic hazard at the surface level is presented in the form of hazard maps for 10% and 2% probability of exceedance in a time frame of 50 years. It is believed that this study will benefit designers and policymakers in building a sustainable city.

2. Regional Tectonics and Seismic Characterization

The seismotectonic features present in the region play a very important role in identifying and categorizing potential seismic source zones and quantifying seismic hazard. The peninsular India which was once considered to be stable has been exhibiting seismic activity at an interesting rate and many researchers have proposed various theories for tectonic stress accumulation and its release over the period. Bott and Dean (1972) explained that the differences in thickness and density distribution in the continental and oceanic crust at the continental margin may generate a stress system favorable to the development of normal faults in the continental crust and thrust faults in the oceanic crust. Sykes (1970) suggested that the high stresses generated by the continental collision between the Indian plate and the Eurasian plate may be very extensive spatially.

Peninsular India is one of the oldest landmasses of the earth's crust formed by the collision of three proto continents such as Singhbhum, Aravalli, and Dharwar with a geological composition involving mainly of Archaean and Proterozoic rocks. The intersection of these three protocontinents is considered to be an active zone for seismic activity. Southern India consists of three major tectonic domains namely,

Dharwar Craton, Eastern Ghat Mobile belt and Southern Granulite terrain. The Dharwar craton is characterized by the Dharwar Schist belt, Kolar Schist belt, and N–S trending Closepet granulite. The average crustal thickness in the Dharwar craton is 35 km with gradual thinning towards the coastal region due to the transition from continental to oceanic crust (Verma and Bansal 2013). The crustal velocity of the upper layers is a key to understanding regional tectonics and evolution of the present day crustal configuration. In this regard, Reddy and Rao (2000) studied the subsurface velocity heterogeneities in the Indian Peninsular Shield. Their findings point out that the Dharwar craton has an average velocity of 5.9–6.4 km/s and 6.8–7.0 km/s corresponding to upper and lower crusts extending to a depth of 22 to 38 km respectively. The velocity in the upper mantle is around 8.1 km/s. The regional strain rates in the stable continental region (SCR) is low in the order of 10^{-10} to 10^{-12} /year. Despite the lower strain rates, the SCR has witnessed damaging earthquakes owing to the presence of numerous critically loaded spatially distributed tectonic features (Seeber et al. 1999).

In order to perform a hazard analysis, a study area within a radius of 350 km (latitude 10.3°N to 16°N and longitude 73°E to 78°E) with Surathkal (near Mangalore) as the center has been chosen (Regulatory guide 1.165, 2008). The part of the region considered for the study is grouped under seismic zone III and the rest in seismic zone II as per IS (1893). The study area is characterized by rugged Malnad region, coastal region, and maidan region. Karnataka has a coastal stretch of 300 km bordered by the Arabian Sea and the Western Ghats. The Western Ghat seismic zone strikes parallel to the west coast of India which was formed by major faulting and uplifting of blocks in the Jurassic period and is suspected to be undergoing adjustments (Radhakrishna, 1993). The studies conducted by Kaila et al. (1972) for the preparation of quantitative seismicity maps suggest that the west coast is more seismically active than the east coast. The major geo-fracture of this terrain is the west coast fault (WCF), which trend NNW, and is considered to be related to the breaking away of the Indian plate from the Gondwanaland (Kayal 2008). Many researchers have asserted Western Continental Margin to be a trailing passive

margin and the part of the West Coast stretching along Karnataka to be transitional in nature.

Mapping of geological features such as faults, lineaments, fractures and shear zones aid in understanding the tectonics and seismicity associated with the region. With the aim of constructing a strong seismic source model to aid in hazard estimation, it is essential to collect all the necessary information on neotectonics, local geology, extension, and movement rates and fault plane solutions. The geological survey of India has studied, identified and mapped the geological features responsible for tectonic activity in India and its surrounding region and has published in the form of a seismotectonic atlas (Dasgupta et al. 2000). This serves as a guide for preparing the seismotectonic map for the study region. The faults and lineaments were georeferenced and digitized from this atlas on the ArcGIS (ESRI 2011) mapping tool platform.

Though a number of geological features have been identified in the study region, there is inadequate information available on the style of faulting and slip rates of each of these features. Further, the seismic activity observed in Peninsular India cannot be attributed to a particular fault or lineament. In other words, the observed seismic activity is distributed and diffused in nature, as a result, direct fault modeling cannot be adopted for the present study. In order to bridge the gap between the potential seismotectonic features and the observed seismicity, seismically active zones are identified. Active zones are characterized by numerous earthquake events with few tectonic features such as faults and lineaments in the vicinity. These active zones are geometrically modeled as areal sources with an assumption that the seismicity is uniform within the zone. This is rather a simplification over a continuously observed seismicity but on the contrary, this method checks the overinterpretation of an earthquake catalog covering a short time window compared to the return period of larger earthquakes (Ashish et al. 2016). Additionally, area source zones accommodate the possibility of the existence of unidentified faults in a study region. The segregation of the study area into a number of potential seismogenic sources (area sources) is accomplished with the aid of seismological, geological, tectonic and geodetic information.

Earlier seismic hazard studies have identified and delineated seismogenic sources based on historical seismicity, geology and tectonic features (Khattari et al. 1984; Bhatia et al. 1999). Gupta (2006) attempted to correlate the tectonic features with the available data on past seismicity and identified 81 potential seismic sources for the whole of India. Seeber et al. (1999) identified 9 potential seismic zones based on observed seismicity and tectonic trends in South India. Nath and Thingbaijam (2012) has recommended areal source zones for India delineated on the basis of seismicity, fault patterns and similarity in fault plane solutions. Kolathayar and Sitharam (2012) identified 104 regional seismic sources based on the pattern of seismic event distribution. The common observation made from all the available literature on seismic source delineation is that the coastal region is considered as a separate seismic zone and in other regions zones are identified based on the fault alignment and spatially distributed seismic events. The seismic zonation adopted in the study attempts to match with the previous hazard studies by considering the focal mechanism observed seismicity and location of faults in the vicinity of the epicenters. The entire study area has been divided into four seismogenic source zones.

Figure 1 represents the tectonic features along with the epicenters of the earthquake events ($M_w > 3$) from the compiled catalog. These events have been temporally categorized into three classes as historic catalog spanning between 1820 and 1900, pre-instrumental catalog between 1901 and 1960 and instrumental catalog between 1961 and 2015. Few of the active faults and lineaments have been labeled and as evident from Fig. 1, there are two trends in the lineaments, one set of lineaments are running parallel to the coast (NNW–SSE) while the other set is transverse to the West coast. A total of five active shear zones, 111 minor lineaments, 10 major lineaments, 15 gravity faults, and around 40 other faults were mapped. Lineaments of length varying from 20 to 475 km were observed. Few active faults and lineaments have been highlighted and explained in the following sections. Figure 2 represents the seismic source zones and the epicenters of the past earthquakes in each of the zones categorized based on magnitude.

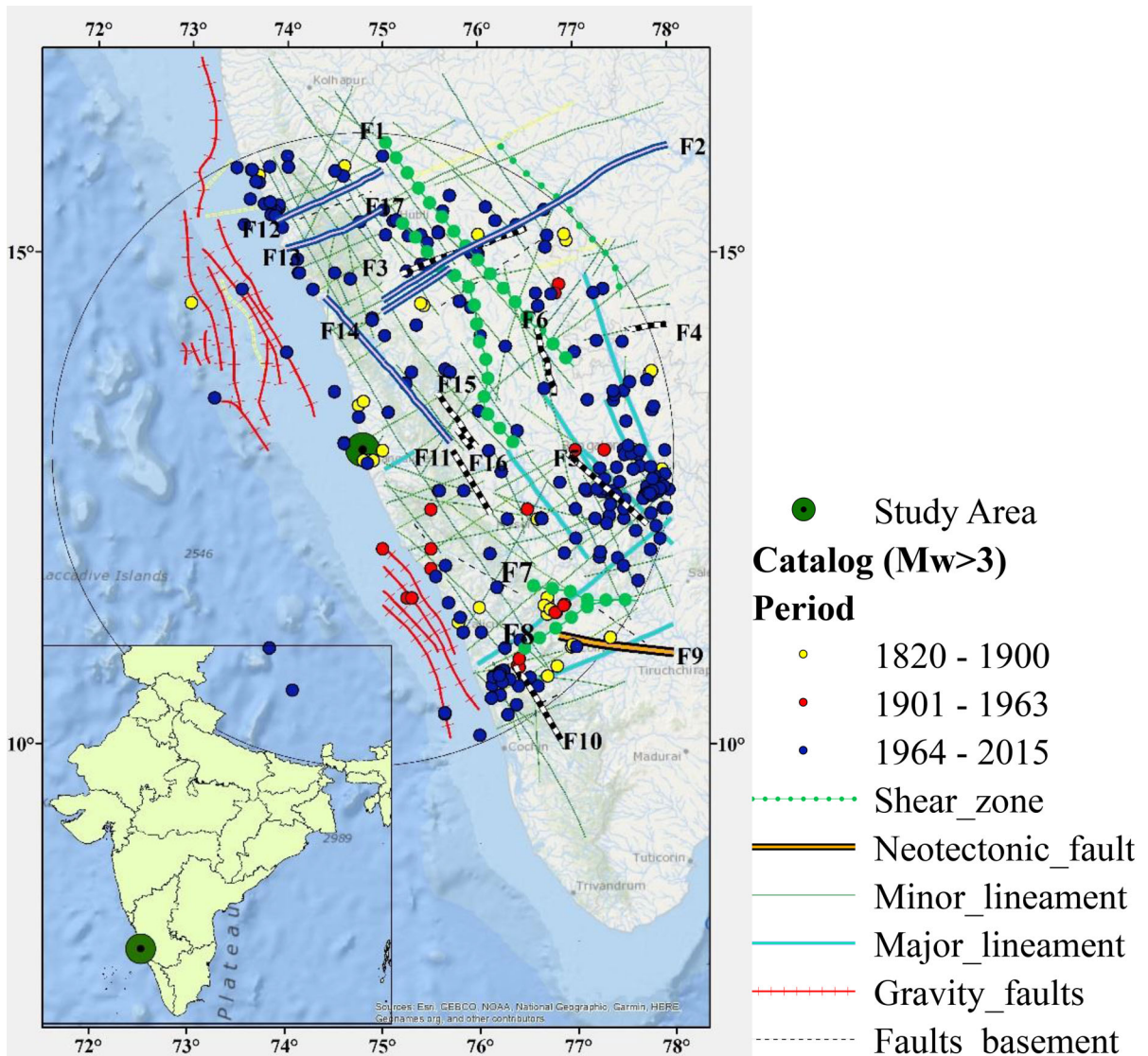


Figure 1

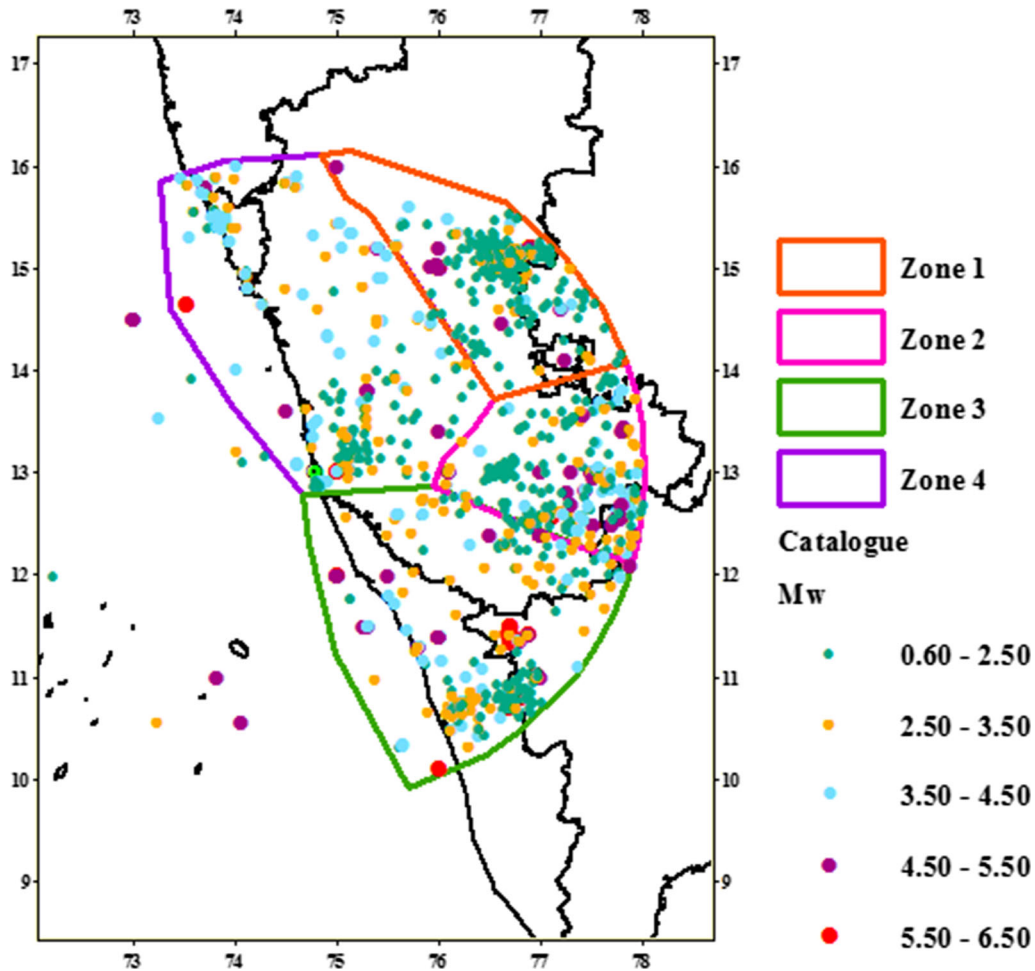
Seismotectonic Map depicting the epicentral location of the historic, Pre-instrumental and instrumental earthquakes ($M_w > 3$) in the study region. The active tectonic features are labeled as F1-Chitradurga Boundary Shear, F2-Chandragutti-Kurnool Lineament, F3-Dharma-Tungabhadra Fault, F4-Bukkapatnam Fault, F5-Arkavati Fault, F6-Chitradurga Boundary Fault, F7-Moyar Shear, F8-Bhavani Shear, F9-Cauvery Fault, F10-Pattikad-Kollengal Fault, F11-Sakleshpura-Bettadpura fault, F12-Mandari Lineament, F13-Benihalla Lineament, F14-Bhadra Lineament, F15-Chikamagalur Fault, F16-Yagachi Fault, F17-Major shear zone

2.1. Tectonics of Seismogenic Source Zones

2.1.1 Seismic Source Zone 1 (SZ 1)

This zone consists of two tectonic features namely Chitradurga Boundary shear (CBS)(F1) of length 345 km and a major shear zone of length 234 km trending in the NNW-SSE direction. The Dharwar

craton is subdivided into Eastern and Western blocks along CBS with intrusive closepet granite occupying the central parts and the majority of the low to moderate earthquakes and a few major earthquakes can be expected along this shear zone. The density and intersection of major lineaments are high over closepet granite and Dharwar group. A total of 351



Seismic source zones along with the epicenters of the past earthquakes grouped into various divisions

events have been reported in this zone and the excessive mining activity being carried out in Bellary and its surrounding area is suspected to be the prime reason for the microseismicity. Earthquake events of magnitude < 3 are usually harmless to the built environment and majority of the rock blasts are within this magnitude range. Hence, the tectonic events and the possible anthropogenic events have been removed. The Bellary earthquake (M_w 5.8) of 1843 felt over a radius of 300 km and epicenters of few moderate-sized earthquakes has drawn the attention of researchers to categorize this zone to be more active in comparison to its surroundings (Gupta 2006; Bhatia 1999). Few seismic events reported post-1960 lie very close to Dharma–Tungabhadra

fault (156 km, F3), Chandragutti Kurnool Lineament (476 km, F2) and Bukkatpatnam Fault (45 km, F4). As a matter of fact, the maximum observed magnitude in the compiled catalog is M_w 6.3 whose epicenter lies in this zone.

2.1.2 Seismic Source Zone 2 (SZ 2)

The geologic composition of this terrain is dominant with granites, gneisses, migmatites, subordinate schists, quartzites, metabasalt, and ultrabasic rocks. This zone encompasses Bangalore and its surrounding rural areas, with its tectonic framework being part of eastern Dharwar Craton. Major tectonic features are Chitradurga Boundary Fault (83 km, F6)

and Arkavathi fault (124 km, F5) along with numerous minor lineaments existing in the zone. An area of low finite strain exists near North of Bangalore between eastern and western supracrustal belts (Balasubrahmanyam 2006). Clusters of earthquake events in the magnitude range of 2.5–5.5 are observed around Bangalore in the vicinity of Arkavathi Fault and east of Mysore summing up to an overall of 295 events. All the events are considered to be tectonic and these clusters of events consist of aftershocks and foreshocks that needs to be carefully removed from the mainshock. The temporal and spatial variation of seismicity in this zone is found to be sporadic. Mandya, Bangalore, and Kolar have been the epicenter for many earthquakes recorded in this region and Ganesh Raj and Nijagunappa (2004) recommends upgrading these areas from seismic zone 2–3 (IS 1893) based on the remote sensing studies. Studies suggest a reverse/normal fault with dominant strike-slip movement rupturing at close intervals to be the main reason behind low to moderate-sized earthquakes in Bangalore. The maximum reported earthquake event is of magnitude M_w 5.6 and studies have suggested that the Killari earthquake (1993) and Sumatra Earthquake (2004) has triggered few investigations of intensity IV in this zone (Sitharam and Anbazhagan 2007). The zone encompasses one of the most densely populated areas such that even a moderate earthquake can cause a great deal of damage.

2.1.3 Seismic Source Zone 3 (SZ 3)

This zone canvases parts of three states namely, Karnataka, Kerala and Tamil Nadu with the major tectonic domain being Pandyan Mobile belt, Khondalite Belt, and a portion of Dharwar craton. Major tectonic features such as Pattikkad Kollengal fault (101 km, F10), Sakleshpur–Bettadpur fault (85 km, F11), Cauvery fault (133 km, F9), Moyar shear (124 km, F7) and Bhavani shear (107 km, F8) encompasses this zone. The N-S trending faults of the Dharwar craton subjected to strike-slip horizontal movements along the Moyar–Bhavani shear zone are speculated to be releasing the stresses accumulated in its interior as a consequence of the Northward movement of the drifting Indian shield

(Valdiya 1989). Studies have revealed the existence of the low-velocity layer in the entire Moyar–Bhavani Shear zone and the region covering these shear zones are interpreted as a collision zone (Reddy and Rao 2000). A total of 329 events have been recorded in this region with the majority of the seismic events having their epicenters around Pattikkad Kollengal fault, Moyar and Bhavani shear. The region between the Moyar and Bhavani shear was observed to be more active with a record of pre-instrumental and instrumental earthquakes. Earthquakes from the instrumental catalog of lower magnitude have been observed near to Sakleshpur–Bettadpura fault. This zone has witnessed seismic events of a wide range varying from the lower magnitude of M_w 1.1 to a higher magnitude of M_w 6.3. Based on the epicentral locations close to a fault, it can be inferred that Cauvery fault and Pattikkad Kollengal fault to be active. The compiled catalog consisting of both pre-instrumental and instrumental catalogs suggests that central midland Kerala as more seismically active in comparison to other parts. The focal mechanism solution from the 67 aftershocks of Idukki earthquake (1988) suggested strike-slip movement on an NW–SE plane implying the association with the pre-existing geological structures (Rastogi et al. 1995).

2.1.4 Seismic Source Zone 4 (SZ 4)

This zone represents the seismic behavior of the coastal region and is characterized by offshore faults and lineaments trending parallel to the coastal line in NNW–SSE direction. However, there exist few lineaments running transverse to the coast such as Chapora, Bennihalla (F13) and Chandragutti Kurnool lineaments in ENE–WSW direction. Gravimetric and Bathymetric studies on the continental margin have confirmed the extension of onshore ENE–WSW and E–W lineaments over a considerable distance into the offshore regions (GSI, 2000). Studies have revealed that the Western continental margin is similar to that of the Eastern margin of the African continent in terms of tectonic and its associated magmatic evolution (Chandrasekharam, 1985). Historic and instrumental earthquakes have been observed along the length of a major shear zone of length 314 km

(F17). Earthquake events of lesser magnitude (M_w 2–3) were observed in the vicinity of Mandari lineament (138 km, F12), Bhadra lineament (224 km, F14), Chikamagalur fault (80 km, F15) and Yagachi fault (29 km, F16). A few historic earthquakes have their epicenters close to the west coast and clusters of events with low magnitude is observed to the west of Bhadra lineament, summing up to about 251 events in the region. Rao (1992) observed that a large number of micro to moderate earthquakes ranging from M_2 to M_5 occur close to 13°N . The occurrence of a large number of small magnitude earthquakes can be attributed to the compression the region is experiencing as a result of continuous seafloor spreading. As the West coast is transitional in character and close to the major shear zones, stress cannot accumulate and hence, released in small amounts resulting in the micro to moderate earthquakes (Subrahmanya 1996). Based on the macroseismic observations and the linear features in this zone, it can be concluded that the geological features are deep-seated structures active along the Western continental margin of India.

2.2. Estimation of Seismicity Parameters for the Compiled Catalog

An updated homogenous seismic catalog complete in all aspects (i.e. date and time of occurrence, epicentral location, magnitude, and focal depth) and free from artifacts and fake events play a major role in characterizing and modeling seismic sources. The study region was considered to be stable and its potential for seismic activity was undermined in the earlier period. As a result, information is available only for significant historic earthquakes in the form of drafted notes, compiled in terms of intensity based on earthquake experiences. The prehistoric events (the 1500 s) were collected from the first Indian earthquake catalog compiled by Oldham (1883). In addition, numerous researchers have studied the tectonics of diverse regions and compiled catalogs by collecting data from various reliable sources. The historic earthquake data was collected from all the regional catalogs compiled by Chandra (1977), Rao and Rao (1984), Srivastava and Ramachandran (1985), Bansal and Gupta (1998), Raj et al. (2001), Rajendran et al. (2009), Martin and Szeliga (2010) and more details about these sources are listed in Table 1. With the advancement of instrumentation in

Table 1

Data sources used in building a seismic source model

Category	References	Scale	Period range	Epistemic uncertainty	Area
Regional and national catalogs	Gangrade et al. (1987)	M_s , M_{ds}	1977–1985	Uncertainty in location	India
	Srivastava and Ramachandran (1985)	MMI	1839–1900	–	India
	Chandra (1977)	MMI, m_B	1618–1975	–	India
	Rao and Rao (1984)	MMI, M , M_L , m_B , and M_s	1751–1984	–	India
	Rajendran et al. (2009)	M_L , MMI	1821–2008	–	Kerala
	Ganesh Raj and Nijagunjappa (2004)	M_w	1828–2001	–	Karnataka
	Raj et al. (2001)	M_w	1821–2001	–	Kerala
	Bansal and Gupta (1998)	M_s , m_B , M_L , M_w	1200–1995	–	India
	Rastogi et al. (1995)	M_s , m_B , M_L , M_w , MMI	1341–2015	–	India
	Martin and Szeliga (2010)	EMS-98	1636–2009	–	India
yengar et al. (2010)	M_w	1200–2008	–	India and surrounding area	
Volumes	Oldham (1883)	Intensity	1500–1869	–	India
	Milne (1911)	Intensity	1600–1900	–	Many

recording earthquakes, the established seismic network has been capable of recording earthquakes of very low magnitude. The instrumental earthquake data (post-1960 s) was collected from various local sources such as Indian Meteorological Department (IMD), Amateur Science Centre (ASC), Geological Survey of India (GSI) and global sources such as National Earthquake Information Center (NEIC), International Seismological Centre (ISC), Incorporated Research Institutions for Seismology (IRIS). The data collected from various sources had listed earthquakes on different Magnitude scales (M_s , m_B , M_L) and Intensity scales (MMI, MSK, EMS-98), which demanded homogenization before further processing. A single earthquake can have more than one valid magnitude and hence, M_s and m_B had to be ruled out as a choice for a standard scale. M_L and M_s exhibit a saturation level at higher magnitudes and are not effective in representing the actual size of an earthquake. However, a scale defined based on the seismic moment, M_w seemed to overcome these disadvantages and was chosen as a standard scale in homogenizing the catalog. In this regard, the region-specific earthquake magnitude scaling relations proposed by Kolathayar et al. (2012) was employed in the interconversion of magnitude scales and a plot of the relationship between different magnitude scales as well as Intensity has been presented in Fig. 3 with

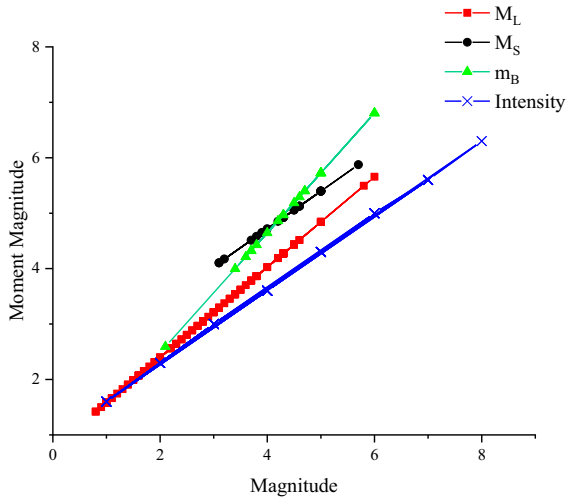


Figure 3

Interconversion of events reported on the various magnitude and intensity scales to moment magnitude scale

the aid of events used in the study. The events reported on the intensity scale was dealt with using the outcome of the studies conducted by Musson et al. (2010). The study involved a comparison of different intensity scales and derived a correlation to convert different intensity scales to the European Macroseismic scale (Grünthal and Wahlström 2012). These events were converted to moment magnitude using the relation given in Eq. 1.

$$M_w = \frac{2}{3}I_0 + 1 \quad (1)$$

The resulting database consisted of certain overlapping earthquake information implying multiple entries of the same event. In the preliminary elimination stage, all the duplicate events were removed based on the accuracy and reliability of the source. In addition, events with their epicenters at a distance farther than 350 km from our main location of interest i.e. Surathkal were excluded. The catalog consists of events occurred over a time span of 190 years starting from the early 1820 s to late 2015 with a total of 1242 events housing a magnitude range of 0.6–6.3. The majority of events have focal depth within 10–15 km from the surface demonstrating the inherent property of intraplate earthquakes being shallow focused. The spatiotemporal plot of the compiled homogeneous earthquake catalog is presented in Fig. 4a. It is evident from the Fig. 4b that the catalog comprises of many artifacts and dependent events such as foreshocks and aftershocks triggered due to static and dynamic stress changes influenced by the main event. In addition, a drastic increase in the number of earthquake events especially in the low magnitude range demonstrates the impact of instrumentation in earthquake monitoring and recording. The period from 1916 to 1933 can be considered as a period of quiescence as none of the sources has recorded seismic activity for this period. The statistical tests on the compiled catalog were performed only for those events of magnitude > 3 with the maximum observed magnitude as 6.3.

The triggered events have been removed from the compiled catalog to fit the Poissonian distribution for the occurrence of earthquakes. The removal of clusters of seismic events based on the spatial–

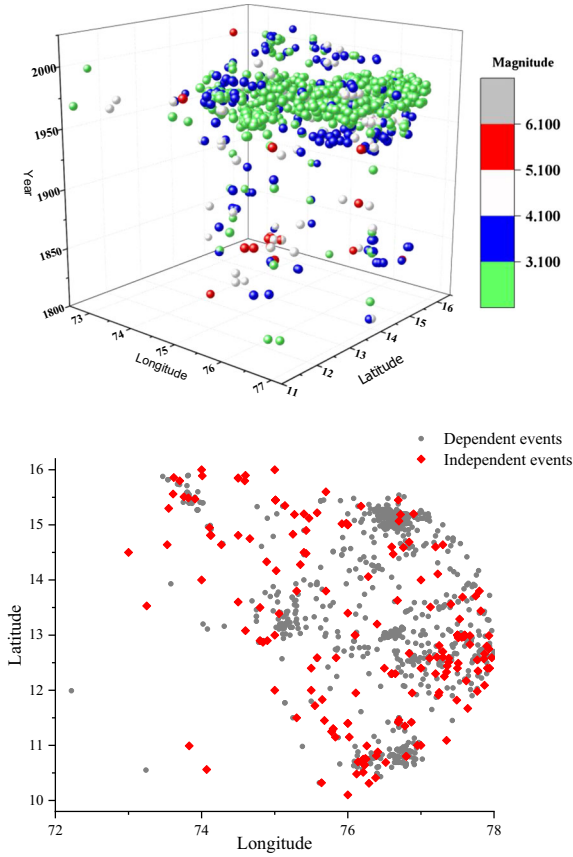


Figure 4

a Spatio-temporal plot of the compiled catalog. **b** Plot separating independent events from dependent events

temporal proximity to one another can be done through various methods, out of which dynamic declustering method has been adopted. Gardner and Knopoff (1974) proposed a declustering algorithm assuming a circular spatial window. The duration of the aftershock sequence, as well as its spatial extent, has been derived as a function of the main shock in the sequence. The algorithm identified that the compiled catalog consisted of 60% (464) dependent events. Figure 4b clearly represents the distinction between mainshocks and dependent events. The declustered catalog was found to be incomplete for different magnitude ranges over different periods. The records of higher magnitude events (above M_w 4.5) were found to be more consistent than that of lower magnitude events. As completeness of a catalog plays a major role in obtaining the seismicity parameters, it was essential to determine the period or

duration in which a magnitude of the certain specified range was found to be completely reported.

The entire catalog has been divided into historical and instrumental catalog depending on the completeness test. The Gutenberg and Richter (1944) proposed an empirical relation to determining the recurrence rate of earthquakes for various magnitude range as given in Eq. 3. The earthquake events reported in each delineated seismic zones were assessed individually to determine the seismicity parameters. Each zone is characterized by a minimum cut off magnitude above which all events are assumed to be reported, the Gutenberg Richter recurrence parameters, observed and estimated maximum magnitude. The details of these parameters for individual zones as well as the entire catalog is given in Table 2.

$$\log \lambda = a - bM \quad (2)$$

λ represents the recurrence rate corresponding to a threshold magnitude M with a and b as the seismicity parameters established from the catalog. The most commonly accepted approach for determining the seismicity parameters is the maximum likelihood approach proposed by Aki (1965) which gives the expression to estimate the 'b' value as follows.

$$\beta = \frac{1}{\bar{m} - m_{\min}} \quad (3)$$

where $\beta = b \ln 10$, \bar{m} is the average magnitude and m_{\min} is the minimum magnitude of completeness. This method can accommodate the uncertainty in the recorded magnitude as well as the incomplete data in the catalog.

A Matlab based computer program (Ha.3) developed by Kijko and Smit (2012) was adopted to estimate the seismicity parameters. Further, the estimated recurrence parameter (mean and quantile distribution) for all the four seismic source zones has been presented in Fig. 5. The seismicity parameters obtained from this study are compared with the studies carried out by other researchers for the same yet wider region and is presented in Table 3. From a statistical perspective, the higher value of 'b' implies that the region is susceptible to a larger percentage of low to moderate-sized earthquakes. However, this can also be attributed to lack of earthquake data and high uncertainty involved in the estimation.

Table 2

Seismicity parameters for the seismic zones and the catalog

Seismic zone	b value	Recurrence rate	M_c	M_{max}
1	0.511 ± 0.083	0.196 ± 0.06	3.5	6.31 ± 0.25
2	0.613 ± 0.11	0.279 ± 0.06	3.5	5.61 ± 0.25
3	0.69 ± 0.043	0.488 ± 0.1	3.5	6.35 ± 0.25
4	0.765 ± 0.078	0.258 ± 0.05	3.5	6.25 ± 0.27

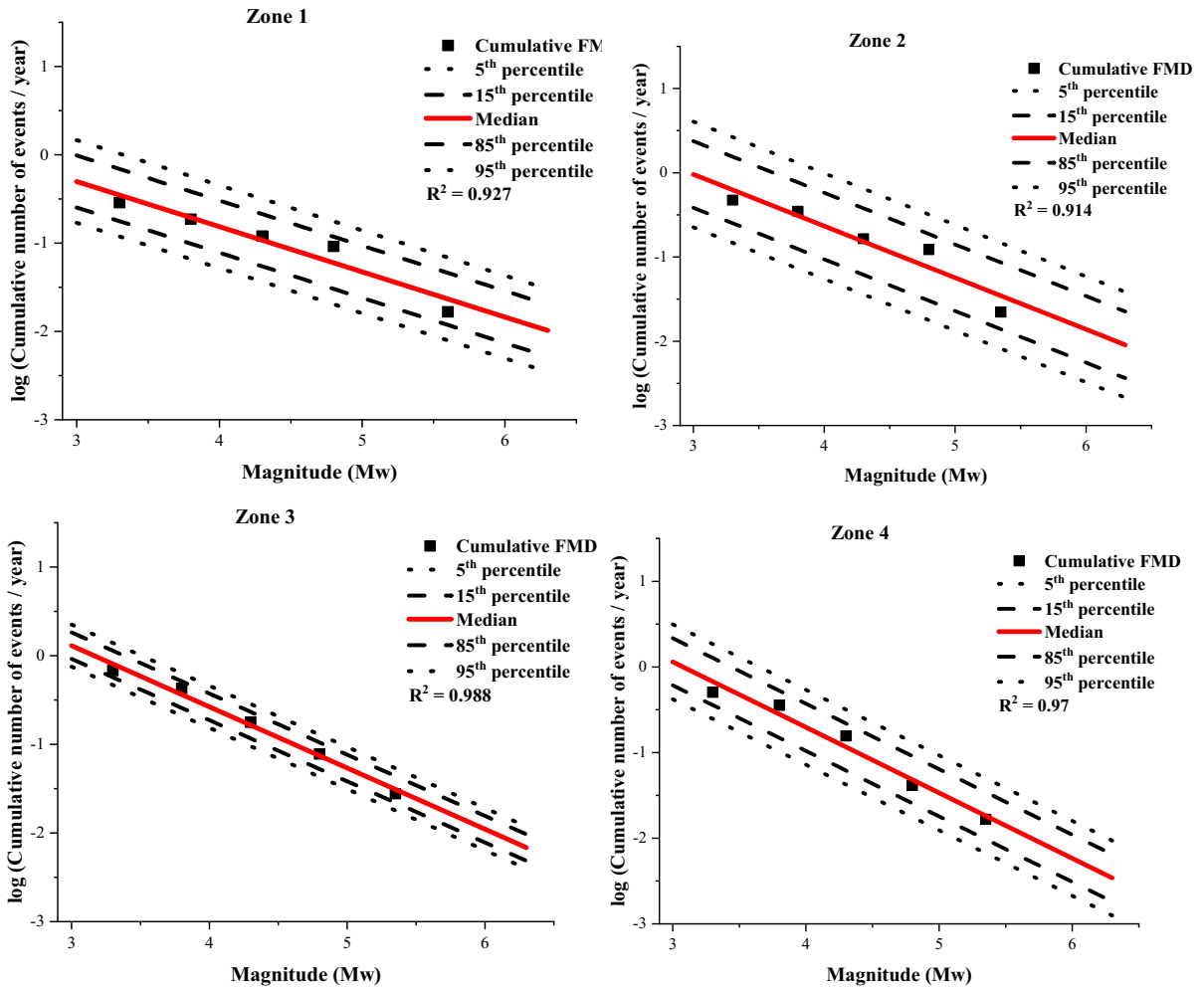


Figure 5
Frequency Magnitude distribution (FMD) of all the four seismic source zones

2.3. Uncertainty in Developing Seismic Source Model

The first essential step in modeling seismicity of a region is to gather all the information and form an exhaustive database related to its associated seismic

activity. In order to achieve this, many kinds of literature on regional tectonics, intensity values, studies on individual earthquakes, previous catalogs, and unpublished materials were scrutinized. The preliminary objective was to compile a regional

Table 3

Comparison of Seismicity Parameters with contemporary studies

Authors	b - value	M_{\max}
Bhatia et al. (1999)	0.598	6.5
Jaiswal and Sinha (2007)	0.92 (\pm 0.052)	6.5
Iyengar et al. (2010)	0.76 (\pm 0.07)	6.8
Kolathayar and Sitharam (2012)	0.57	6
Ashish et al. (2016)	0.85	6.5
Present study	0.74 (\pm 0.08)	6.3 (\pm 0.5)

catalog that includes the most recent events not listed in the previously published material that is free from duplications and fake events. Due to the lack of recording instruments in the earlier period, the historical part of the catalog relies on many regional and national catalogs. Table 1 lists the sources used in the study for constructing a seismic source model. While adopting the data, the sources were chosen in such a way that the catalog is publicly available and its sources are referenced. Priority was given to those catalogs listing events estimated from regional studies and those reported on M_w scale. The major drawback when adopting events from multiple sources is duplication. When multiple recordings of the same event are providing contradictory information, those dataset providing events values in terms of magnitude is chosen. However, the historical events are mostly reported on intensity scales and hence, requires special attention. These events need to be validated through multiple sources (such as previously compiled catalogs, studies on individual earthquakes and the seismicity studies of various regions). In the present study, only those historical events reported in many of the previously compiled catalogs and published reports related to seismicity of Peninsular India have been considered.

There is a great deal of uncertainty involved in the location of the events, its depth, and magnitude. Gangrade et al. (1987) suggest the error in locating an earthquake to vary across India in the range of 0.01° to 0.09° . Srivastav and Ramachandran (1985) excludes the data from the published catalogs and provides a database consisting of events extracted from microfilms of Times of India, Statesman, and Hindu. Priority is given to those catalogs that account for the uncertainty in the reported magnitude. However, in the absence of uncertainty, a default value of

0.5 has been chosen for prehistoric events and 0.25 for historic events and those M_w values obtained from Intensity conversions. Majority of the historic events lack focal depth information and in those cases, a default value of 10 km has been chosen. Further, there are certain events in the catalog which have not been verified by multiple sources due to lack of data. Therefore, the compiled catalog consists of year, month, date, and time of occurrence of events along with the information on its location, magnitude or intensity, and focal depth. To account for the uncertainties involved in estimating the b-value, a bootstrap method with 100 bootstraps was implemented. (Chernick 1999).

In the compiled catalog it was observed that the completeness of events is homogeneous only for a certain time period. Catalog completeness is a function of the magnitude and substantially varies from region to region (Grünthal and Wahlström 2012). The entire catalog has been divided into two parts namely, Historical catalog and Instrumental Catalog. The Instrumental catalog has been derived from various global agencies and hence assumed to be complete. The uncertainty in these events is considered to be 0.1. In order to accommodate the epistemic uncertainty involved in estimating the recurrence relation, a logic tree was constructed sampling into 5 branches as shown in Fig. 6. Quantile distribution has been adopted for estimating the G–R recurrence parameters and each branch has been given suitable weights. These seismicity parameters are derived independently for each individual zones and the uncertainty in estimating M_{\max} has been addressed by considering $M_{\max(\text{obs})}$, $M_{\max(\text{obs})} + \Delta$ and $M_{\max(\text{obs})} + 2\Delta$. The weighting factors for M_{\max} has been chosen based on the history of seismic activity and regional tectonics. The uncertainty in estimating the maximum magnitude for the entire study region has been chosen as observed $M_{\max(\text{obs})} + 0.5$ (Iyengar et al. 2010) as shown in Table 3. The whole of the study area belongs to the same tectonic regime and the source depth is considered to be 10 km and hence, the epistemic uncertainty has not been considered for these two parameters. The inadequate information on the tectonic activity in the study area necessitates the choice of area source model and the uncertainty involved in the delineation

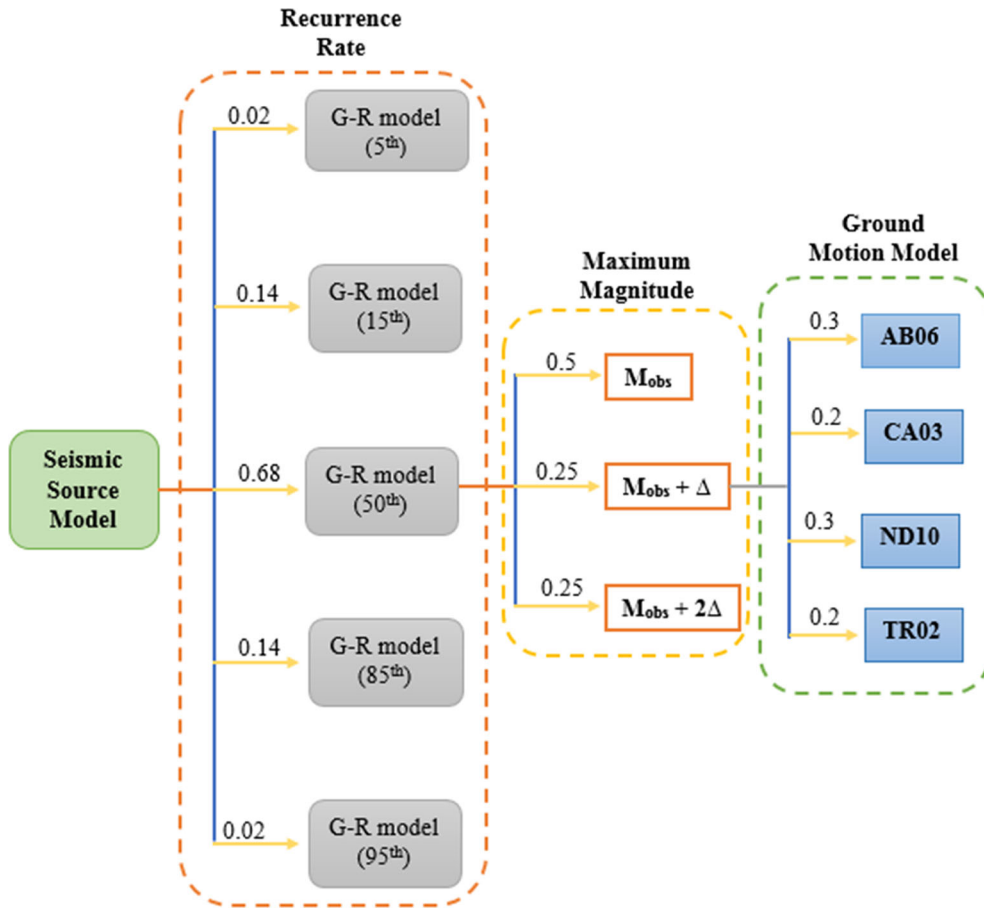


Figure 6

Logic tree representing the earthquake rate model, maximum magnitude, and ground motion models

of these areal seismic sources has not been addressed in the study. The outcome of this approach accounts for various earthquake scenarios and uncertainties in estimating the seismicity patterns, completeness of events, the maximum magnitude. These results serve as an input in predicting the ground motion for various exceedance probabilities in a given time frame.

3. Selection of Ground Motion Prediction Equations

The estimation of seismicity parameters provides an overall idea of the potential earthquake magnitudes and its location. The main focus lies in understanding the ground motion that can be expected at the site, which is predicted using Ground

Motion Prediction Equations (GMPEs), also known as ground motion models developed by performing statistical regression on a large database of observed ground motion intensities. GMPEs anticipates the ground motion in terms of intensity measures (PGA, PSA, etc.) as a function of magnitude, distance, faulting mechanism, near-surface site conditions and so on. Due to the lack of strong ground motion data in India, appropriate attenuation laws developed for the regional conditions are scanty. During the investigation of aftershocks of Bhuj earthquake, Cramer and Kumar (2003) found that the regional tectonics of peninsular India (PI) is similar to that of Eastern North America (ENA) and the GMPEs developed for ENA are comparable with PI.

The ground motion prediction equations developed for a similar tectonic regime i.e.

stable continental region has been considered for preliminary testing. The criteria for selecting GMPEs as suggested by Bommer et al. (2010) was used for the initial screening process. The study region is characterized by low to moderate seismicity and consequently poor in terms of strong motion data. As a result, the data-driven testing methods were not applicable to the present scenario. However, qualitative testing of the applicability of the GMPEs to regional condition was validated by using macroseismic observations of Bhuj and Jabalpur earthquake given by Singh et al. (2003) as shown in Fig. 7. The distance (R_{JB}) of the recorded macroseismic data ranges from 91 km to 603 km and it is to be noted that few of these observations are beyond the applicable distance range of various GMPEs (ND10, RI07,

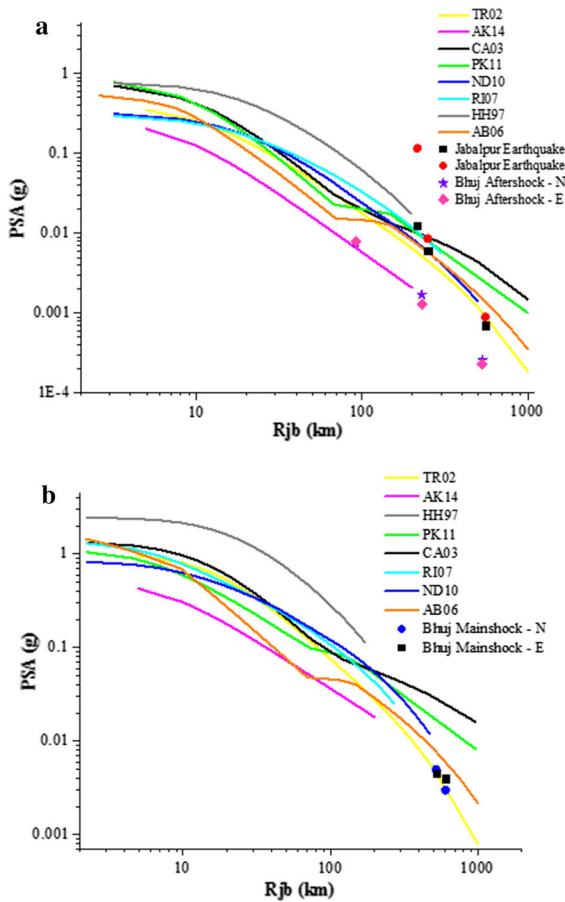


Figure 7

Comparison between the GMPEs and the macroseismic recordings during **a** Jabalpur (1997) earthquake and Bhuj aftershock ($M_w = 5.7$) and **b** Bhuj (2001) ($M_w = 7.6$)

AK14, TR02, HH97). Usually, extrapolation is adapted to compute the ground motion parameter (PGA, PSA) at distance beyond the applicable range. However, these extrapolations may add on to the existing uncertainty in the estimated value and hence, not encouraged. Table 4 lists the GMPEs along with their characteristics investigated in the present study out of which four of them were chosen. The attenuation equation suggested by Toro et al. (1997) and later modified as Toro (2002) (abbreviated as TR02) was found to provide a nearly exact estimation for Bhuj main shock and a reasonable prediction for Jabalpur earthquake. TR02 was developed for hard rock site condition characterized by an average shear velocity of 1828 ms^{-1} . Raghu Kanth and Iyengar (2007) (abbreviated as RI07) and Iyengar et al. (2010) are the equations developed for regional data. The former provides a higher estimate while the latter predicts a rational value, as a result, Iyengar et al. (2010) (abbreviated as ND10) was chosen for the study. Further, RI07 is applicable for a shorter distance range and ND10 is the improvised version of this ground motion model. Hence, RI07 has not been considered to avoid duplication of GMPEs. ND10 was developed for Type A sites and the A type reference site has been defined as layers of a variety of rocks summing the average value of $V_{S(30)} > 1500 \text{ ms}^{-1}$. The database chosen for deriving the equation suggested by Akkar et al. (2014) mainly comprises of events from a relatively active region and hence, was found to be irrelevant for the present study region in addition to smaller distance range. Atkinson and Boore (2006) modified as Atkinson and Boore (2011) (abbreviated as AB06) and Campbell (2003) (abbreviated as CA03) was developed for Eastern North America and was observed to provide lower and upper bound estimates respectively for the intended macroseismic data. AB06 developed ground motion relations for hard rock sites in ENA (near surface shear velocity $> 2000 \text{ ms}^{-1}$ or NEHRP A) as a function of moment magnitude and closest distance to the fault rupture. This ground motion prediction model incorporates the seismographic data with a magnitude range of 5–7.5 with distance less than 200 km in providing median and standard deviation values for the ground motion parameters (S_a for 5% damped,

Table 4
 GMPEs investigated in the study

Region	No. of records	No. of events	Mw	R type	R range (km)	Component	Period(s)	Style of faulting (stress drop parameter)	Site effect	Vs 30	Acronym	GMPE
Eastern North America	Stochastic finite fault model		3.5–8	Rrup	1–1000	PSA, PGA, PGV	0.01–5	140 bars	Vs30	2000 ms ⁻¹	AB06	Atkinson and Boore ^a
Eastern North America	Hybrid empirical method		5–8.2	Rrup	1–1000	PGA, PSA	0.01–4	105–215 bars	Vs30	2800 ms ⁻¹	CA03	Campbell ^a
Eastern North America	Simulated data		5–7.5	Repi	1–200	Sa, PGA	0.01–3	100–200 bars	Vs30	3500 ms ⁻¹	HH97	Hwang and Hwo
India	Stochastic finite fault model		4–8.5	Rhyp	1–500	Sa, PGA	0.01–4	100–300 bars	Vs30	1500 ms ⁻¹	ND10	Iyengar et al. ^a
Peninsular India	Simulated data		4–8.0	Rhyp	1–300	Sa, PGA	0.01–4	100–300 bars	Vs30	3600 ms ⁻¹	R107	Raghu kanth and Iyengar
Eastern North America	Hybrid empirical method		5–8.0	Rrup	1–1000	PGA, PSA	0.01–10	250 bars	Vs30	2000 ms ⁻¹	PK11	Pezeshk
Central and Eastern North America	Stochastic ground motion model		5–8.0	Rjb	1–500	Sa, PGA	0.01–2	120 bars	Dummy variable	1828 ms ⁻¹	TR02	Toro ^a
Europe and middle east	1041	221	4–7.6	Rjb	1–200	PSA, PGA, PGV	0.01–4	N, R, S	Vs30	150–1200 ms ⁻¹	AK14	Akkar

^aGMPEs finally selected for estimating the seismic hazard

PGA, PGV). CA03 developed ground motion model by hybrid empirical method incorporating differences in stress drop, source properties, crustal attenuation, regional crustal structure. This empirical attenuation relation is considered to be most appropriate for estimating the ground motion on ENA hard rock with a shear-wave velocity (V_s) of 2800 m/s for earthquakes of magnitude $M_w \geq 5.0$ and $R_{rup} \leq 70$ km. However, it has been extended to larger distances using stochastic ground motion estimates. Pezeshk et al. (2011) (abbreviated as PK11) predicts a higher PGA and PSA values at shorter distances when compared with the rest of the equations and was opted out of the study. Hwang and Hwo (1997) (abbreviated as HH97) provides a reasonable estimate but the applicable distance range is too small and would lead to extrapolation with a higher degree of uncertainty. The ground motion model developed for the study consists of multiple GMPEs along with its inherent aleatory and epistemic uncertainties developed for both global and regional data.

In hazard applications, the non-data driven methods or quality testing methods must be supported by trellis plots and sensitivity analysis (Danciu et al. 2016). Trellis plots are prepared to capture the distribution of ground motion estimates in multidimensional space (M, R, Spectral Period). Trellis plots are presented in three Figs. 8, 9 and 10. Figures 8 and 9 consists of 10 panels and Fig. 9 consists of 12 panels. Each panel represents a specific earthquake scenario and demonstrates the nonphysical behavior of the attenuation equation. All the GMPEs adopted in this study have developed its own database for the ground motion model incorporating stochastic finite-fault rupture and hybrid empirical methods. Each of these GMPEs has been developed on the different distance scales and they were converted to R_{JB} using the scaling relation developed by EPRI (2004).

The attenuation of GMPEs for a various magnitude distance combination has been presented in Fig. 8. AB06 predicts a lower bound value for all the scenarios whereas ND10 is on the upper bound. For shorter distance (i.e. $R_{JB} = 10$ km) the spectral shape of all the equations remains to be the same but this trend observes a significant period shift in achieving maximum PSA values at far off distances (i.e.

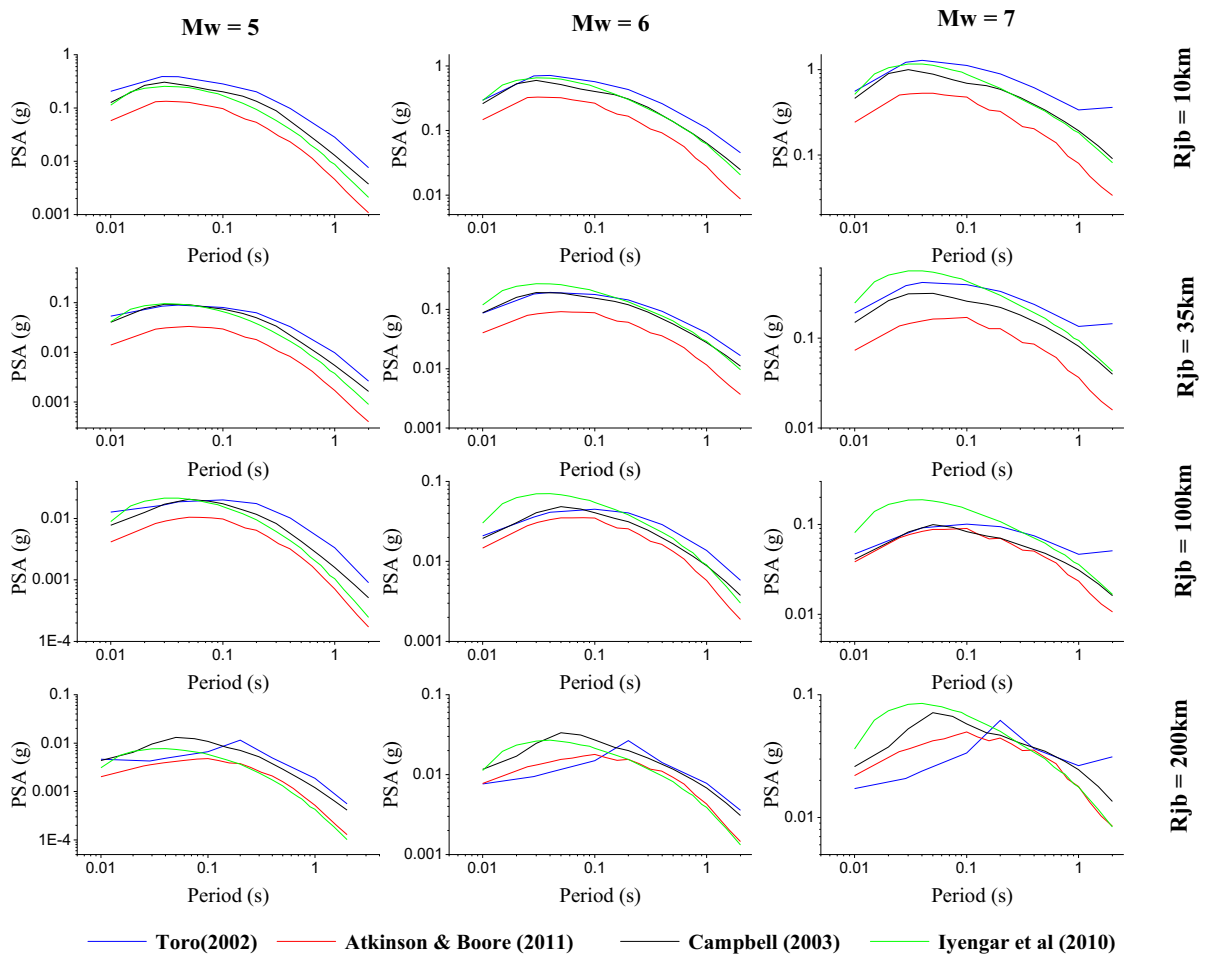


Figure 8

Trellis plots for various earthquake scenarios in magnitude-Source to site distance space for varying spectral period

$R_{JB} = 200$ km). ND10 demonstrates a well-pronounced peak at larger distances but around the same period range, which is also the case with CA03. AB06 and TR02 witnesses a drastic shift in the period for maximum PSA for higher magnitude and longer distance. This distinctive behavior among GMPEs may be attributed to the difference in their functional forms as well as the data used in developing the equation. TR02 exhibits magnitude saturation at higher magnitudes i.e. $M_w = 7$. Figure 9 represents the magnitude dependent attenuation of the GMPEs considered in the study. TR02 and ND10 represent anelastic attenuation at distances beyond 70–100 km and results in steep attenuation. These equations are quite favorable as they can be applied to a wider magnitude-distance range of interest. AB06 exhibits

steeper attenuation for PGA at all magnitude ranges but this feature is not so evident at longer spectral periods thereby demonstrating distance saturation. CA03 predicts upper bound values and exhibits distance saturation in all the earthquake scenarios. The magnitude saturation as a function of distance and the spectral period has been presented in Fig. 10. AB06, CA03, and ND10 exhibit magnitude saturation but the same are not evident in TR02. From all the trellis plots combined together, it can be concluded that AB06 provides a lower bound estimate and CA03 provides an upper bound estimate. In many instances, AB06 and ND10 demonstrate a similar behavior and TR02 toggles between lower and upper bound values along a varied range of magnitude distance combination. The performance of various GMPEs under

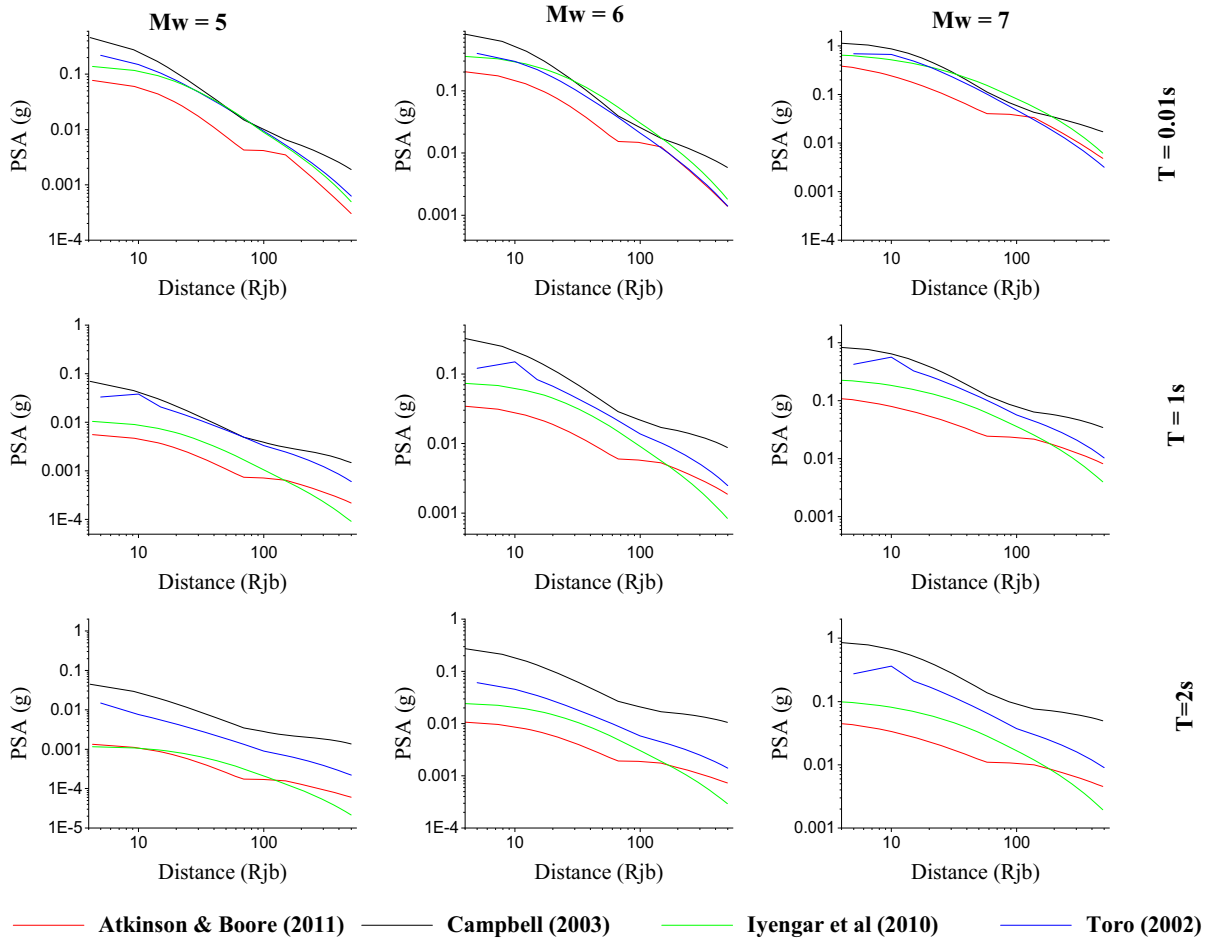


Figure 9
Trellis plots for various earthquake scenarios in magnitude-spectral period space for a varying source to site distance

different earthquake scenario guides in choosing the weighting factors for logic tree combination.

3.1. Uncertainties in Ground Motion Prediction model

The uncertainties involved in the formulation and execution of a ground motion prediction model can be categorized as aleatory and epistemic uncertainties. Epistemic uncertainty represents the lack of knowledge in understanding and modeling the complex earthquake phenomena. This issue can be overcome with improved data and knowledge such as incorporating multiple ground motion models. These are combined using a logic tree approach with the weighting factors for each model representing the

confidence in its prediction as shown in Fig. 6. Aleatory uncertainty represents the natural randomness in earthquake occurrences and cannot be reduced but can provide reasonable estimates with additional data. The impact of aleatory uncertainty in the prediction of ground motion is represented by epsilon ' ϵ ', a fraction of the standard deviation ' σ ' of a GMPE. Studies have recognized that the inclusion of σ leads to higher hazard estimates and alternative models influence the overall behavior of the equation. In other words, the aleatory uncertainty controls the shape of the hazard curves while epistemic uncertainty leads to multiple hazard curves equivalent to the logic tree end-branches (Bommer and Abrahamson 2006). While assigning the weights to each of these branches, it was made sure that each of these

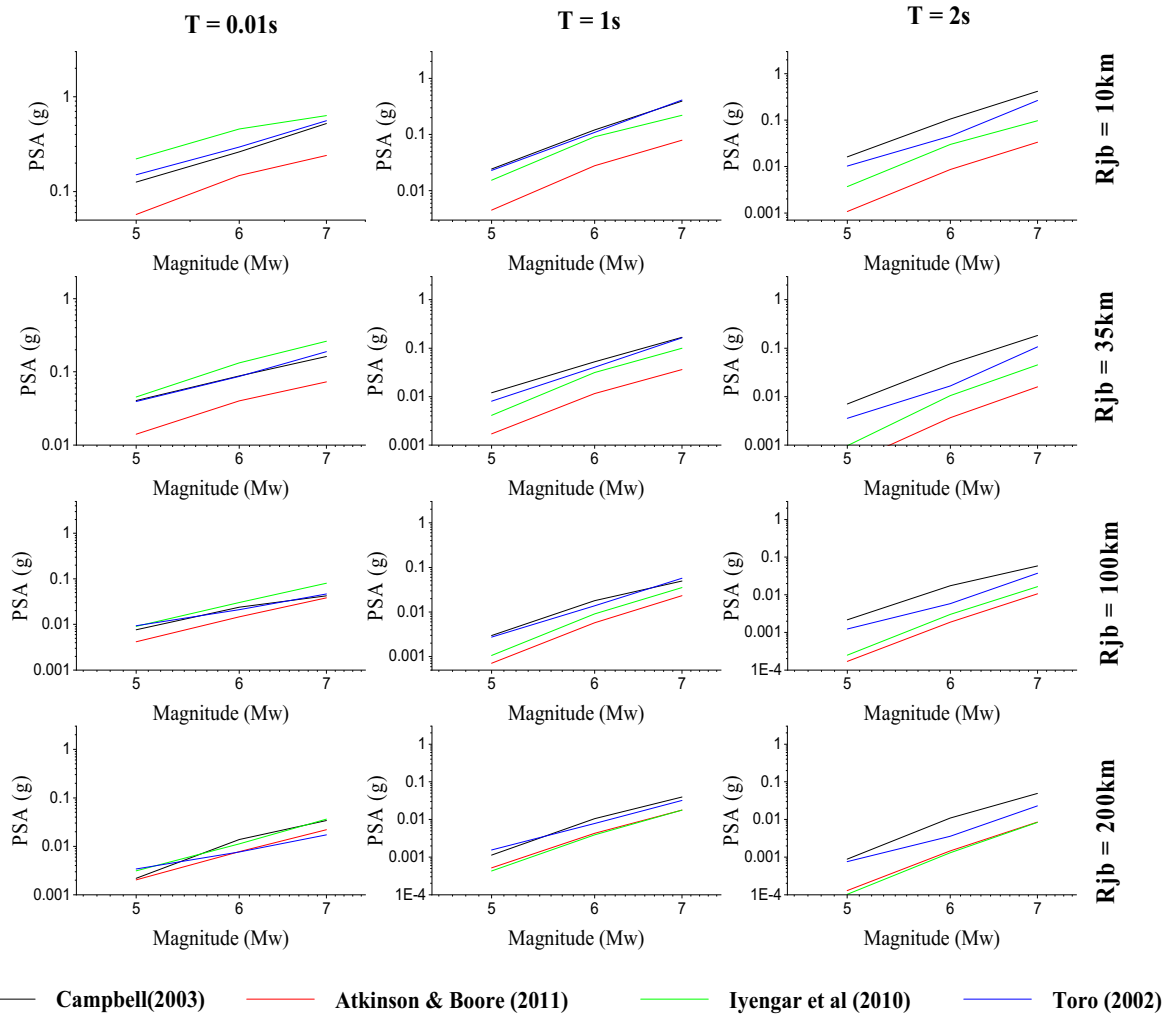


Figure 10

Trellis plots for various earthquake scenarios in the spectral period-source to site distance space for varying magnitude range

equations is mutually exclusive and collectively exhaustive, with the summation of weights of all the branches from a common node being equal to one (Bommer and Scherbaum 2008). The choice of weighting factors for ground motion models is aided by the trellis plots and sensitivity analysis. The performance of various ground motion models with various weighting factors is analyzed and an appropriate combination is chosen and presented as the final estimate.

The aleatory uncertainty is included in the attenuation equation at the modeling stage and each GMPE treats this uncertainty in a different manner. For instance, TR02 has the most sophisticated

modeling for aleatory and epistemic uncertainty. Despite the fact that the equation uses 20 year old data TR02 is the most widely accepted ground motion model for stable continental shield region. It represents the lack of data in the form of epistemic uncertainty. The total aleatory uncertainty in the model is considered to be magnitude and distance-dependent whereas epistemic uncertainty is considered to be magnitude dependent alone. The aleatory uncertainty models inter-event variability, stress drop, focal depth, Kappa and Q. Further, the attenuation equation proposed includes variables for aleatory and epistemic uncertainty. CA03 is based on the hybrid empirical method which accommodates

aleatory and epistemic uncertainty in the predicted ground motion. The aleatory uncertainty is modeled as lognormal distribution and the values of standard deviation for various magnitude, distance, and spectral period ranges are provided along with the proposed GMPE. Further, the aleatory uncertainty has been included in the proposed equation as a function of magnitude. AB06 includes aleatory uncertainty in the model parameters within the simulation. The epistemic uncertainty considers the stress parameter alone and these uncertainties are modeled as a normal distribution function. ND10 presents a set of values along with the coefficients for the attenuation equation facilitating in plotting mean and mean + sigma values for a region.

In addition to these inherent uncertainties, it is equally important to maintain compatibility among the chosen equations. In other words, different GMPEs produce predictions in terms of different variables (PGA, PSA, SA) using different distance metrics (R_{JB} , R_{hyp} , R_{epi} , R_{rup}) corresponding to different soil conditions. While choosing GMPEs and combining them in a logic tree special attention should be given to these influential parameters. The ground motion models adopted in the study computes the ground motion parameter corresponding to reference sites of distinct shear velocities ($V_{s(30)}$) such as 1500 ms^{-1} (ND10), 2000 ms^{-1} (AB06), 2800 ms^{-1} (CA03), 1828 ms^{-1} (TR02). However, NEHRP categorizes sites with $V_s > 1500 \text{ ms}^{-1}$ as site class 'A'. As a result, in the present study, the hazard has been computed at the bedrock level corresponding to NEHRP site class A. However, there are methods that can adjust GMPEs to a site-specific velocity profile using regional data such as Edwards et al. (2016). Further, the availability of nonlinear site-specific information can better enhance the prediction through direct inclusion in hazard computation with input motions defined directly at the bedrock level (Bommer et al. 2017).

4. Estimation of Seismic Hazard at Bedrock Level

The probabilistic approach for seismic hazard assessment accommodates all the seismic sources in the study area and predicts the hazard in terms of

probability of exceedance for a given intensity level and a predefined time frame. The seismic hazard for the study area has been estimated at the bedrock level ($V_s > 1500 \text{ ms}^{-1}$) by incorporating the seismicity parameters estimated for each of the identified seismogenic source zones along with the attenuation characteristics using the computer program CRISIS 2015. Each source zone is characterized by minimum and a maximum magnitude and their recurrence parameters. For an area source model, the software assumes a uniform Poissonian distribution of seismicity (i.e. the occurrence of earthquakes in a region is independent of the previous earthquakes for the same region) over the entire source. The software uses a triangulation procedure to discretize the area sources and this discretization is continued until one of the criteria is achieved. The criteria are minimum triangle size (S) and the ratio of the minimum site to source distance to triangle size (R) and the user has complete flexibility to input these values. As a part of the sensitivity analysis, various combinations of these controlling parameters i.e. S and R were evaluated. However, no significant differences were observed in the hazard values except that the computation time increases with an increase in the values of S and R and a similar observation has been made by Danciu et al. (2010). Initially, each source with 'N' vertices is divided into N-2 triangles and further subdivision continues until the S or R-value specified by the user is achieved. These subdivisions are performed by means of a recursive function. The site to source distance is measured from the computation site to the centroid of the triangle. The seismicity of the area source is assigned to the center of each triangle. CRISIS uses spatial integration procedure as explained above to sample seismicity source model and predict hazard accounting for all possible locations of the earthquake within the source. The results of the hazard analysis are presented in the form of hazard curves, uniform hazard spectrum, and deaggregation plots. The hazard curves are plotted for Mangalore city (12.81°N , 74.87°E) for various spectral periods as shown in Fig. 11 and it is clear from Fig. 11 that for a given exceedance probability higher acceleration values can be expected up to 0.5 s. Few important cities from each seismic zones were chosen and their respective uniform hazard

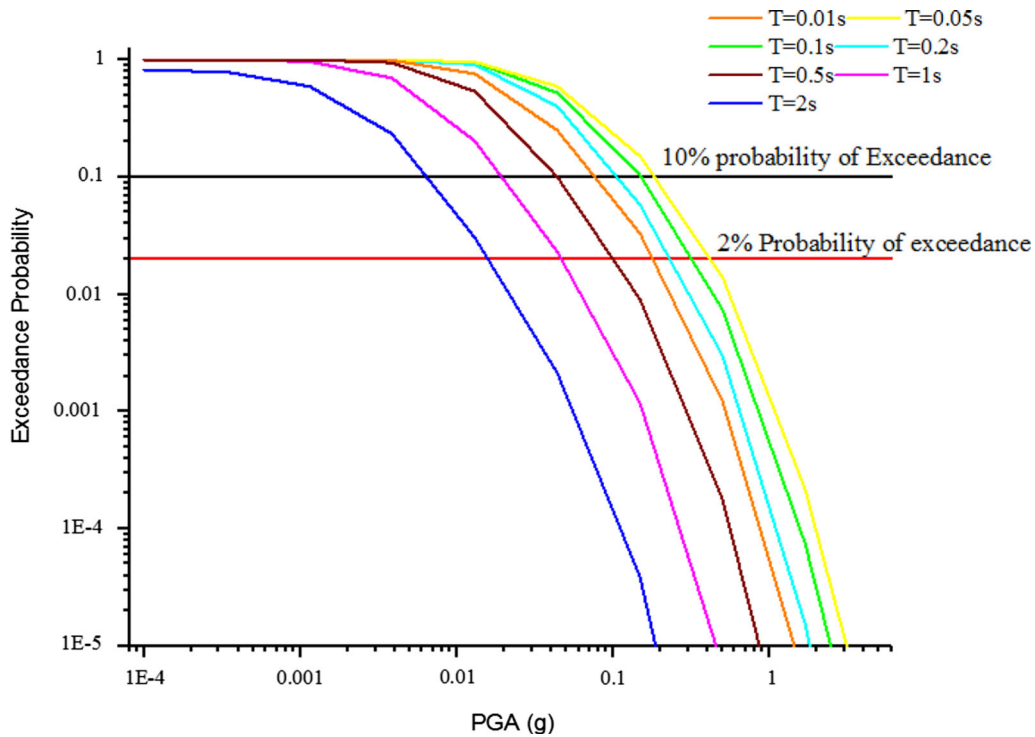


Figure 11
Hazard curves for Mangalore city for varying spectral periods in a time frame of 50 years

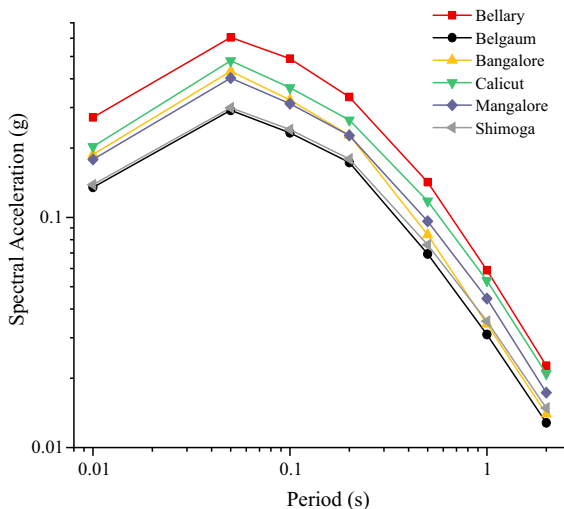


Figure 12
Uniform Hazard Spectrum for various important cities at the bedrock level ($V_s > 1500 \text{ ms}^{-1}$) for 2% probability of exceedance (return period-2475 years)

spectrum has been plotted in Fig. 12. Bellary (15.13°N, 76.92°E) lies in seismic zone 1 demonstrating the highest acceleration values followed by

Calicut (11.25°N, 75.78°E) lying in zone 3. The hazard curves have been plotted for the bedrock condition for various exceedance probabilities in a time frame of 50 years. The uniform hazard spectrum (UHS) has been plotted for 2% probability of exceedance (return period = 2475 years) in 50 years. The seismic hazard maps for the study area have been plotted and presented in Fig. 13 for 10% and 2% probability of exceedance corresponding to bedrock level conditions.

The PGA values estimated at the bedrock level are compared with the predictions made by various researchers for three different regions as listed in Table 5. Jaiswal and Sinha (2007) performed seismic hazard for Peninsular India using zoneless approach and this study uses GMPEs which have been superseded by a more recent and sophisticated ground motion models. Further, the study was almost a decade ago thereby creating space for improved knowledge and additional data in recent years. However, the hazard predicted for Bangalore seems to be in good agreement with that of the present

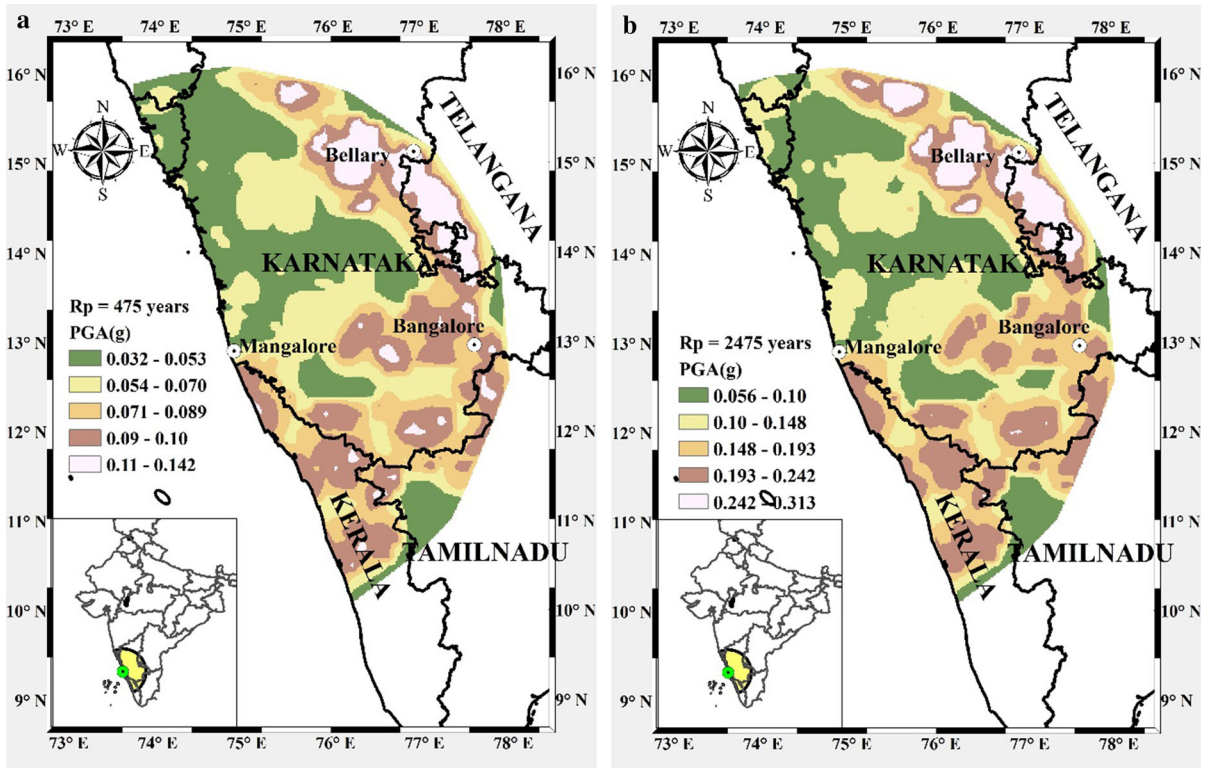


Figure 13

Seismic Hazard Maps representing PGA for the study area at 10% (a) and 2% (b) probability of exceedance at the bedrock level condition

Table 5

Comparison of hazard values predicted for different regions

Intensity levels	Bangalore	Mangalore	Bellary	Authors	Site class
10% probability of exceedance	0.095	0.076	0.112	Present study	$V_s > 1500 \text{ ms}^{-1}$
	0.131	0.044	0.064	Sitharam et al. (2012)	Bedrock
	0.024	0.023	0.038	Iyengar et al. (2010)	NEHRP 'A'
	0.05	0.08	0.05	BIS (2016)	Rock/stiff soil
	0.11	0.08	0.12	Nath and Thingbaijam (2012)	B-C boundary
	0.10	–	–	Jaiswal and Sinha (2007)	Hard rock
	0.06	0.1	0.08	Sitharam and Kolathayar (2013)	$V_s > 1500 \text{ ms}^{-1}$
	0.057	0.06	0.10	Ashish et al. (2016)	$V_s > 1100 \text{ ms}^{-1}$

estimation and the city wise predicted PGA values are not available for improved discussion in the matter. Iyengar et al. (2010) predict relatively lesser values for all the considered region corresponding to NEHRP site class A. The study adopts areal source zones and makes use of regionally developed GMPEs for different parts of the country. This was the first attempt to develop a common attenuation equation with spatially varying coefficients for each identified individual tectonic regime. However, the major

limitation of this study is the use of single GMPE making epistemic uncertainty dominant in the hazard prediction. Sitharam et al. (2012) performed both deterministic and probabilistic seismic hazard analysis for Karnataka state alone by adopting linear and areal source models for PSHA. The study underestimates the seismic potential of both Mangalore and Bellary and slightly overestimates for Bangalore. The attenuation equation used in the study has been superseded by a more recent publication and is

believed to be the reason for the difference in the predicted values with that of the present study. Nath and Thingbaijam (2012) have adopted the smoothed gridded seismicity model as well as the uniform seismicity areal source model. A major coincidence with this study is the use of a similar trend in areal source delineation and same GMPEs but with varying weighting factors for each GMPE. Ashish et al. (2016), and Nath and Thingbaijam (2012) demonstrated the seismic potential of Bellary to be higher than the other two locations supporting the results obtained in this study. Ashish et al. (2016) used multiple source models such as areal source, gridded seismicity model and fault source model to estimate the seismic hazard for entire Peninsular India. The computed hazard values match well with that of the present study except for a slight underestimation for Bangalore region. The difference in the predicted hazard values from the present study and that of Sitharam and Kolathayar (2013) is quite significant and the reason behind this difference is due to the use of single GMPEs by the latter. Overall, the present study is believed to have produced a rational estimate of the seismic hazard values by incorporating the available datasets on earthquake events and regionally applicable ground motion models.

5. De-Aggregation of Seismic Hazard

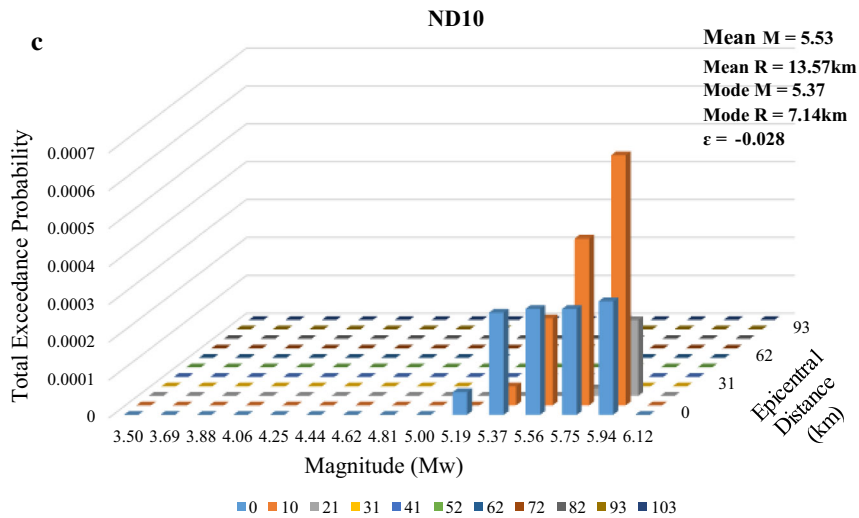
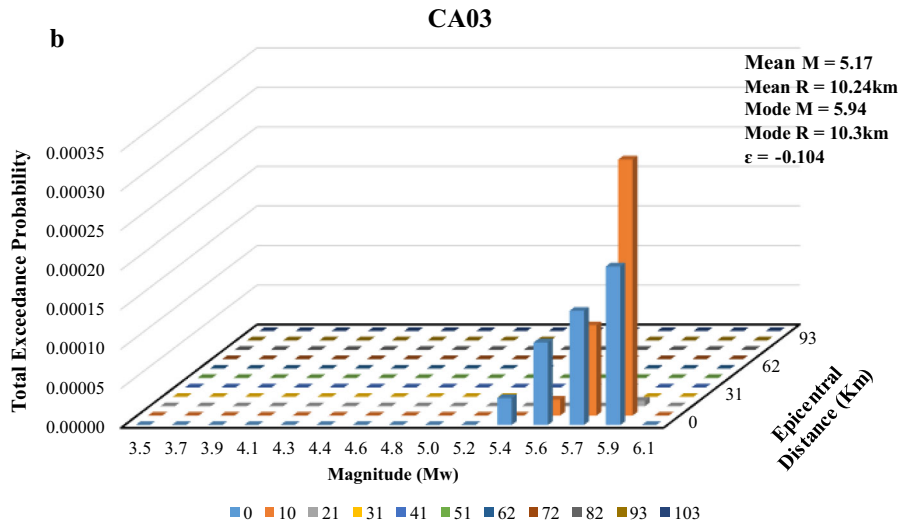
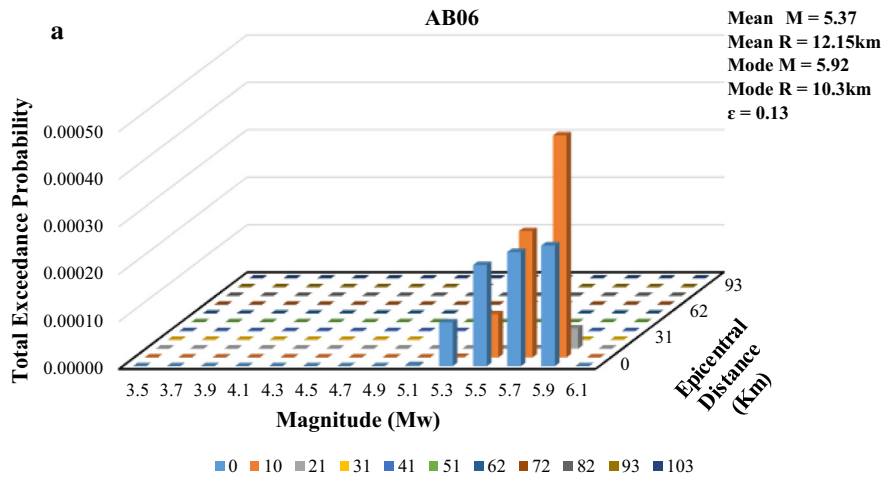
PSHA integrates all the possible earthquake scenarios (magnitude–distance) and predicts the hazard level but difficult to identify the relative contribution of the seismic sources for a chosen site of interest. In order to obtain the specific scenario earthquake (combination of magnitude, and distance) contributing to the specified hazard level, de-aggregation of the seismic hazard is mandatory. The de-aggregation of the computed seismic hazard provides better insights into the significance of various influential parameters contributing to hazard (Bazzurro and Cornell 1999). The investigation of the most influential earthquake scenario consists of three essential parameters such as magnitude, distance, and epsilon. These three parameters have a significant influence on the exceedance probability. De-aggregation was performed using CRISIS and the program provides

Figure 14

a De-aggregation plot for AB06 with intensity 0.121 g for 2% probability of exceedance. **b** De-aggregation plot for CA03 with intensity 0.229 g for 2% probability of exceedance. **c** De-aggregation plot for ND10 with intensity 0.17 g for 2% probability of exceedance. **d** De-aggregation plot for TR02 with intensity 0.177 g for 2% probability of exceedance

flexibility to the user to input the intensity level or the probability level (i.e. 2% or 10% probability exceedance), time frame (say 50 years), magnitude, distance, and epsilon. Epsilon (ϵ) represents the measure of the contribution to hazard above or below the mean predicted value. The contribution of the smallest earthquakes is significant when $\epsilon > 1$ and for larger earthquakes $\epsilon < 1$ (Halchuk et al. 2007). For a chosen range of M, R, ϵ the de-aggregation plots represents the probability of exceedance as a percentage of total exceedance probability (for all magnitude, distances and epsilon equal to $-\infty$) (Aguilar-Meléndez et al. 2017). In a stable continental region such as the present study area, the contribution comes from a wide range of magnitudes and distances. In order to capture the importance of small earthquakes at close distance to large earthquakes at far off distance, mean M and R-value were chosen from de-aggregation plots. The ϵ value was calculated as the number of standard deviations by which the target ground motion deviated from the median value predicted from a GMPE for a given M and R (Bazzurro and Cornell, 1999). The de-aggregation plots for each GMPE have been presented in Fig. 14a–d. AB06 provided relatively lower estimates throughout the study and highlights the importance of moderate-sized earthquakes (M_w 5 to 6) at smaller distances ($R_{epi} < 25$ km). Additionally, the impact of an M_w 6 earthquake up to 50 km distance has been well demonstrated. CA03 provides an upper bound estimate and recommends that an M_w 6 earthquake has a significant impact only till 30 km. The possible reason for this estimation is the higher magnitude range (M_w 5–8.2) incorporated in the modeling phase of the GMPE. ND10 provides a reasonable de-aggregation accommodating the significance of earthquakes ($M_w > 5$) at distances with 20 km and for events with M_w 6 up to 50 km. This GMPE is derived from the regional data and is expected to best represent the local attenuation characteristics.

Probabilistic Seismic Hazard Assessment of Mangalore and Its Adjoining



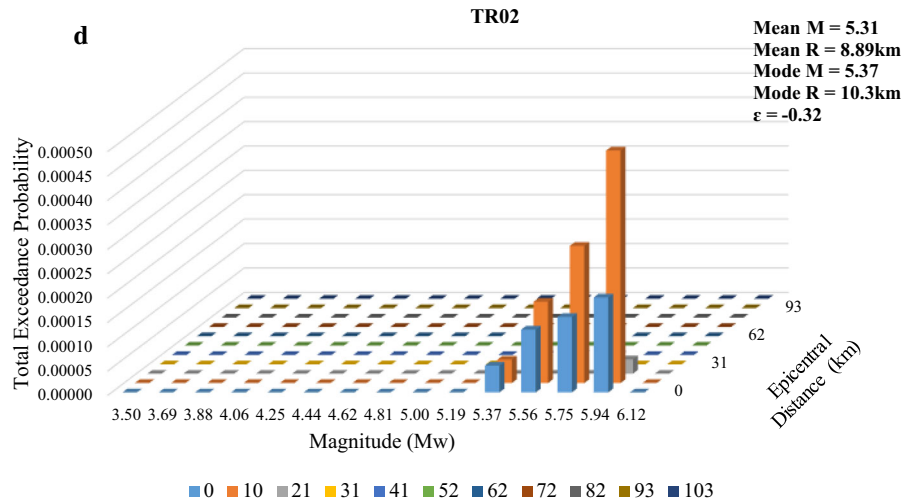


Figure 14
continued

Further, it shows increased exceedance probability for increasing magnitude and near source distances. TR02 highlights the significance of lower magnitude events at a near-source distance (< 10 km) and higher magnitude events ($M_w > 6$) at distances greater than 30 km. In conclusion, all the GMPEs highlight the importance of near-source effect irrespective of the size of an earthquake event but larger magnitude events can cause a significant impact at far off distances say 50 km. In general, de-aggregation is carried out to determine controlling earthquakes consistent with the uniform hazard spectrum to generate time histories that are representative of the target hazard level. These time histories can be used for various engineering purpose and in this study these results are used in selecting ground motions for site response analysis.

6. Sensitivity Analysis of Input Parameters to Seismic Hazard

The key to a factual estimation of seismic hazard lies in the accuracy of the methods that define the input parameters to the best of the available knowledge. There are two major inputs for seismic hazard estimation and they are seismic source model and ground motion prediction model. Each model has its own step by step formulation process with multiple

approaches available for each of these processes. This section first describes the various methodologies adopted in constructing a seismic source model followed by the Ground motion prediction model.

6.1. Earthquake Data Preparation

6.1.1 Declustering Algorithm

The earthquake data collected from various sources are usually reported on the different magnitude and intensity scales. To compile a regional catalog, the first step is to homogenize all the events to a single scale and in the present study, M_w has been chosen as the standard. The collected data consists of many dependent events which need to be removed so that that earthquake recurrence rate fits the Poissonian distribution. In other words, the occurrence of an earthquake is independent of the past earthquakes in the same region. In this regard, many declustering (removal of clusters of events) algorithms are available such as window method, cluster method and stochastic Declustering. The present study adopts a window method based on the available information about the earthquakes and the regional tectonic data. There are two types of window methods namely, static and dynamic window methods. The static window method assumes a fixed time window from the main shock for identifying the aftershocks.

However, dynamic window methods adopt a magnitude dependent time and distance window to identify the dependent events. In this approach, two declustering algorithms suggested by Gardner and Knopoff (1974) and later modified by Uhrhammer (1986) were compared.

The algorithm for Gardener and Knopoff is given as

$$D = 10^{0.1238*M+0.983} \text{ (Km)} \quad (4)$$

$$T = \begin{cases} 10^{0.032*M+2.7389} & \text{if } M \geq 6.5 \\ 10^{0.5409*M-0.547} & \text{else} \end{cases} \text{ (days)} \quad (5)$$

The algorithm for Urhammer is given as

$$D = e^{-1.024+0.804*M} \text{ (Km)} \quad (6)$$

$$T = e^{-2.87+1.235*M} \text{ (Days)} \quad (7)$$

The compiled catalog was subjected to both the declustering algorithm and the comparison has been shown in Fig. 15. The declustered catalog from Urhammer was found to have artifacts with poor quality control and the estimation based on this catalog may carry erroneous results. The catalog from Gardener and Knopoff exhibited a better removal of dependent events (about 60% of the collected data were identified as dependent events). Hence, Gardener and Knopoff Declustering algorithm was used in the study.

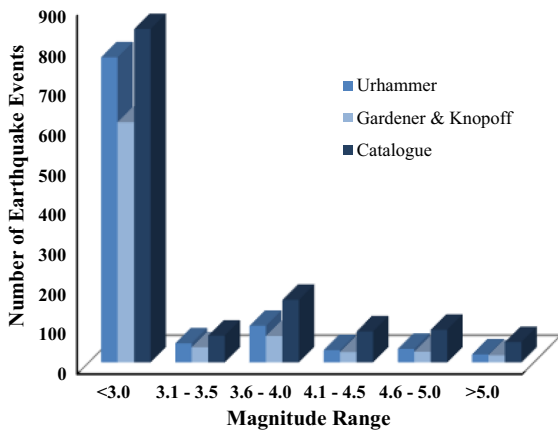


Figure 15

Comparison of the declustering algorithms with the compiled regional catalog

6.1.2 Completeness of the Compiled Catalog

The completeness magnitude (Mc) is the lowest magnitude in the catalog above which all the earthquake events recorded in a space–time frame are exhaustive. It is crucial to have a factual estimation of Mc, as an estimate on the higher end might lead to scraping off of the usable data due to undersampling while on the lower end might provide erroneous analysis of the seismicity parameters due to incomplete data sets.

Magnitude of Completeness can be computed in two ways, namely,

- Catalog-Based Method
- Network-Based Method.

The catalog based method is a straightforward approach where the analysis and computation are performed on the compiled catalog data whereas the network-based method is quite complex and time-consuming. The latter method is applicable only to the instrumental data which is available for the last 5–6 decades. Hence, the former method is used in the study. Under catalog based method, different approaches are available to determine the Mc as well the completeness period for various magnitude range. The present study uses a statistical method to manually calculate the completeness period and this method was suggested by Stepp (1972).

Stepp’s Method:

Determination of magnitude of completeness through an empirical and statistically simple method based on the stability of magnitude recurrence rate was introduced by Stepp (1972). In this method, the entire catalog is grouped into different magnitude classes similar to the previous method with an interval of $\Delta M = 0.5$ and each magnitude class is modeled as a point process. The cumulative number of events in each individual magnitude class is determined for the different time window. The cumulative annual rate of earthquakes is calculated starting from magnitude 3. For a particular magnitude range, let $\times 1, \times 2, \dots, \times R$ be the number of events per unit interval, obtained from the catalog. The unbiased estimate of the mean rate per unit time interval of this sample is

$$x = \frac{1}{N} \sum_{i=1}^n x_i \quad (8)$$

where N = number of intervals.

And its variance is given as

$$\sigma_x^2 = \frac{x}{T} \quad (9)$$

This method is based on the assumption that the occurrence of earthquakes follows a stationary Poisson's process. The completeness test performed using Stepp's method has been presented in figure. The completeness period of magnitude classes 3.1–3.5, 3.6–4.0, 4.1–4.5, 4.5–5.0 and > 5.0 are found to be 40, 60, 70.80 and 160 years respectively. The completeness test performed using the described method has been presented in Fig. 16.

6.1.3 Computation of Gutenberg–Richter Recurrence Parameters

The completeness test serves as a key for estimating the region dependent recurrence parameters. There are various computer programs that are available for estimating the magnitude of completeness (M_c) and the G–R recurrence parameters such as ZMAP, Ha3 and so on. ZMAP by Wiemer (2001) estimates M_c through various methods such as Maximum curvature technique (MAXC), Entire Magnitude Range (EMR) with an option to bootstrap the samples. A well-

detailed explanation about each of these methods is available in Woessner and Wiemer (2005). In the present study, the manually estimated M_c was compared with that of the value obtained from the program. The program estimated G–R parameters were found to be in good agreement with that of the manually calculated values. The statistical method explained earlier has been superseded by a more robust method for estimating the seismicity parameters. Maximum likelihood approach is the most widely used method and the computer program Ha3 adopted this technique for estimating the seismicity parameters. Based on the results from the Stepp's method the entire catalog has been divided into the historical catalog and instrumental catalog. The seismicity parameters estimated using this method were also found to be in good agreement with the manual calculations and hence, further estimation was done using maximum likelihood method. The estimated b-value for zone 1 and zone 2 was found to be very less in the range of 0.5–0.65 hinting, influence of low magnitude events ($M_w < 3$) in fitting G–R parameters. Evidently, a large number of events in zone 1 lies in the magnitude range of 2–3 (M_w) and b-value are sensitive to the magnitude of completeness (M_c). Upon investigation of low magnitude bins, b-value was found to be as high as 0.95 ± 0.13 for an M_c of 2.2, demonstrating the dominance of lower magnitude events. However, such smaller events are insignificant in hazard estimation and are screened out when events with $M_w > 3$ are considered.

6.1.4 Seismic Source Modeling

The delineation of seismic source zones plays a major role in quantifying the seismic hazard for a region. In this regard, multiple configurations of the area source zones were investigated. The delineation process considers multiple parameters such as tectonic regime, source depth, fault plane solutions and, seismic activity. The whole of the study area belongs to the same tectonic regime i.e. the stable continental region with shallow focussed earthquakes. The zones of weakness and the predominant focal mechanism have been identified in the Peninsular region only after the occurrence of destructive earthquakes and

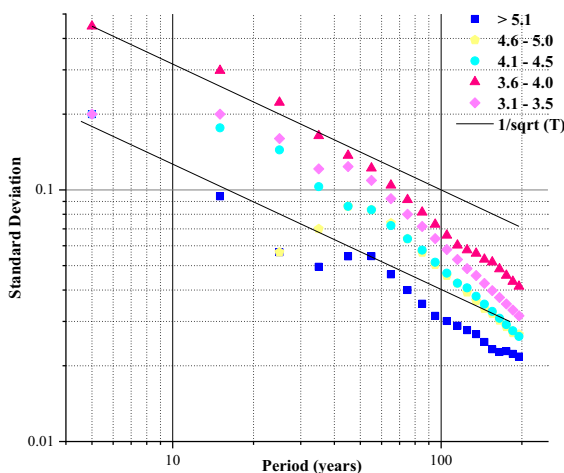


Figure 16
Completeness test for the declustered regional catalog using Stepp's method

the majority of the studies points towards fault plane solution of strike-slip nature. However, few studies revealed the existence of a normal/reverse fault near Bangalore with a dominant strike-slip movement and hence, it has been separately delineated as seismic zone 2. From the seismotectonic perspective, the entire study region falls under two major tectonic domains i.e. Southern Granulite terrain (SGT) and Dharwar craton. The SGT has been modeled separately as seismic zone 3 in the present study whereas the other three zones belong to Dharwar Craton. During catalog compilation, focal depth for the majority of seismic events was not available and upon careful examination of the previous hazard studies, the focal depth has been chosen as 10 km. Majority of the seismic hazard assessment projects at the National level have modeled the coastal tract as a separate seismic zone and within the Peninsular the delineation has been performed based on the observed seismicity and fault alignment. The seismic delineation strategy adopted in the study aims to identify the seismic source zones at a smaller scale while matching with the large-scale seismic source zonation of the earlier studies. The areal sources were chosen for modeling seismicity due to lack of data on individual faults as well as suspecting the existence of unidentified faults in the study region. Hence, the seismic source model adopted in the study attempts to capture diffused seismicity. The alternate configurations of area sources have not been provided due to space constraints. Bhatia et al. (1999) suggested that the Indian shield can be considered as one single seismic source zone for hazard computation and smaller seismic zones can be identified based on locales of major earthquakes and lineaments. As a result, the validation for the chosen area source configuration has been provided by considering the entire study area as a single zone. However, it is believed that the spatial variation of seismicity parameters may not be effectively captured in a single seismic source zone and hence, this source model is used solely for the purpose of validation. The comparison of a single source model and the adopted area source model has been presented in the form of seismicity characteristics as shown in Fig. 17.

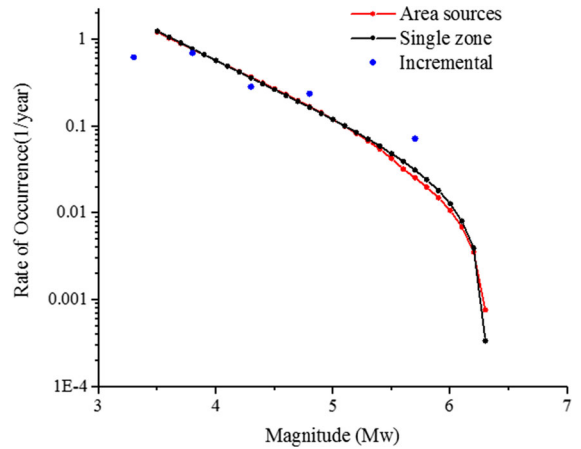


Figure 17

Comparison of G-R recurrence parameters derived for the catalog data and the summation of all the area sources

6.2. Ground Motion Prediction Model

Selection of ground motion prediction equations has been explained in the earlier section. The sensitivity of the weights assigned to each GMPEs in logic tree combination in estimating intensity values has been investigated in this section. The epistemic uncertainty involved in the choice of GMPEs is addressed by selecting multiple models and combined using a logic tree. The weights assigned to each of the GMPE requires expert judgment considering their performance in qualitative testing and trellis plots. Based on these criteria different combinations of GMPE has been investigated as shown in Table 6. The results of the trellis plots clearly indicated that CA03 forms the higher end and AB06 form lower end of the hazard estimation. However, ND10 tends to balance and provides a median estimate among the chosen 4 GMPEs. The logic tree combination 2 provided higher estimates as CA03 and ND10 as a higher weighting factor as shown in Fig. 18a. The

Table 6

Details of logic tree established for sensitivity analysis

GMPE	LT-1	LT-2	LT-3	LT-4	LT-5
AB11	0.3	0.2	0.25	0.2	0.3
CA03	0.2	0.3	0.25	0.2	0.3
ND10	0.3	0.3	0.25	0.2	0.2
TR02	0.2	0.2	0.25	0.4	0.2

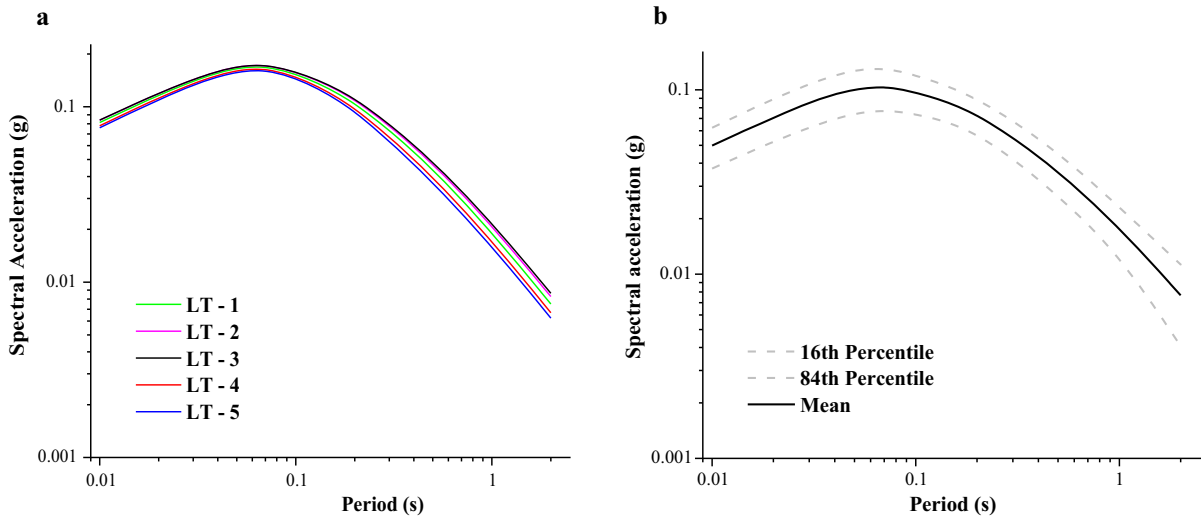


Figure 18

a Median uniform hazard spectra obtained from various logic tree combinations and **b** Mean and percentile estimation of uniform Hazard spectrum for the chosen logic tree combination (LT-1)

combination 3 provides equal weighting factors to all the GMPEs which was in good agreement with that of combination 2. The combination 5 provided an unreasonably lower estimation owing to the lesser weighting factors for ND10 and TR02. On the other hand, a higher weighting factor was provided for TR02 in combination 4. However, this combination suggested that TR02 alone is insufficient in predicting the overall seismic hazard. The choice was to be made between combinations 1 and 3. CA03 gives higher estimation in all the considered scenarios as exhibited in trellis plots. In addition, it underestimates the significance of low magnitude earthquakes in de-aggregation. Hence, CA03 had to have a least weighting factor. TR02 is for a higher magnitude range and hence, was given a lesser weighting factor. ND10 is derived based on the regional data and performed exceptionally well in qualitative testing as well as de-aggregation. The equation accommodates anelastic attenuation, accounts for exceedance probability of low magnitude events and impact of large earthquakes at far off distances. AB06 provides a significant lower bound estimation in the majority of the scenarios considered but the study region is characterized by low to moderate seismicity. Hence, providing more weighting factor to other attenuation equation would lead to unrealistic estimates of

intensity values. Hence, combination 1 was chosen for the final seismic hazard assessment. The median and percentile uniform hazard spectrum estimated from the chosen logic tree combination 1 has been depicted in Fig. 18b.

7. Seismic Site Characterization Using Topography

The seismic waves propagating from the source located at a depth towards the surface undergoes significant modification due to impedance contrast in the underlying soil layers termed as local site effect. The local geology and the soil profile underlying a structure has the potential to cause extensive damage. The predicted seismic hazard captures the ground motion at the bedrock level and this needs to be further investigated in order to understand the near-surface attenuation/amplification characteristics. The site amplification characteristics can be determined through indirect measurements such as shear velocity and dynamic shear modulus of the supporting subsoil. Various in situ methods are available to determine the site-specific shear velocity profile but may always not be feasible due to inaccessibility of the sites or lack of favorable conditions for testing. In such scenarios, it is desirable to adopt a methodology applicable to any

region ruling out the major drawback of in situ testing methods. An alternate method using topographic slope as a proxy for seismic soil conditions was applied in our study and is widely applicable to any region as the elevation data is available at a uniform sampling for the entire globe. Allen and Wald (2009) identified the contribution of surficial geology to the amplification of ground shaking. They suggested that the topographic variations as an indicator of near-surface geomorphology and lithology to the first order, with steep mountains indicating rock, nearly flat basins indicating soil and a transition between the end members as intermediate slope. This is based on the premise that more competent material (high velocity) are more likely to maintain steep slopes whereas deep basin sediments are deposited primarily in environments with very low gradients. They have developed a correlation between the Topographic gradient and $V_s(30)$ measurements and the same has been compared with the results of other countries such as Taipei, Australia and so on in proving the versatile applications of the correlation. The applicability of this method was tested by Lemoine et al. (2012) for Europe and the Middle East by performing novel statistical methods. The results concluded that the correlation suggested by Allen and Wald (2009) can be used for National or regional first order studies in the absence of detailed information. However, for sites located in small basins, flat-lying volcanic basins or coastal locations the slope has to be calculated considering bathymetric data as well.

In our study, the digital elevation model (DEM) corresponding to a resolution of the 1 arc minute with a combination of topography and bathymetry was considered for generating a slope map. The data was obtained from the ETOPO1 global relief model developed by the National Oceanic and Atmospheric Administration (NOAA) (Amante and Eakins 2009). The data was resampled to 30 arc second before generating the slope values. The slope value at the center of each grid of size approximately $1 \text{ km} \times 1 \text{ km}$ was obtained using ArcGIS v 10.1 (ESRI 2010) which was further used for seismic site characterization. The applicability of the correlation was tested by comparing the mean slope values obtained for Mississippi embayment and the entire continental US east of the rocky mountains which are

physiographically similar to the present study region. The slope range values observed in our study area is 0.036–0.055 for higher topographic relief and 0.0017–0.02 for lower relief. These values are in good agreement with that of Allen and Wald (2009) and hence, the slope correlation developed for the stable continental region was applied. These correlations were revised with higher resolution data (9 arcs second data) by Allen and Wald (2009). However, the increased resolution leads to smoothing of the minor perturbations losing the actual representation of the physical changes in the flat-lying region where it is crucial due to significant amplification. Hence, 30 arc second data has been used in the present study.

These slope values indirectly contribute to the $V_{s(30)}$ measurements that are determined by the correlation and the $V_{s(30)}$ map for the study area is as shown in Fig. 19. The majority of our study area is classified under NEHRP site category D and the Western Ghats and other hill stations such as Nilgiris, B R hills are grouped under site class B and C. The identification of site classes based on the shear

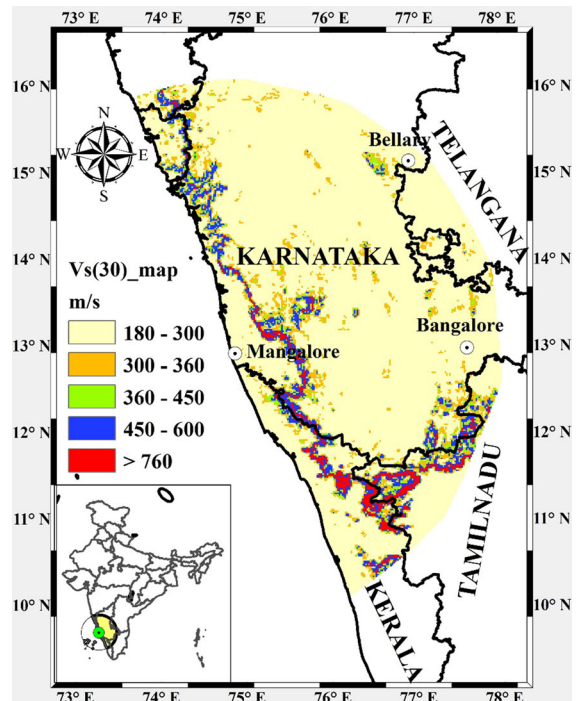


Figure 19

$V_{s(30)}$ map generated from the slope values for the study area

velocity is helpful in computing site amplification factor for each individual site category. The resulting surface level ground motion visualized as bedrock motion modified by the soil layers and the site coefficient essential in this estimation was generated from the Eqs. (7) and (8), adapted from Raghu Kanth and Iyengar (2007).

$$\ln F_s = a_1 y_{br} + a_2 + \ln \delta_s \quad (10)$$

$$y_s = y_{br} * F_s \quad (11)$$

The site coefficient F_s is estimated for each site class encountered in our study area using the regression coefficients a_1 and a_2 with an error δ_s . The regression coefficients vary for each site class and the site coefficient is a function of time used to modify the bedrock motion according to its overlying site. Figure 20 represents the comparison of the response spectra generated at the bedrock level, surface and that obtained from BIS (1893). It is clearly evident from Fig. 20 that the codal provision underestimates the seismic hazard of the study region. In addition, significant spectral amplification is observed in the period range of 0.05–1 s which happens to be the natural frequency of most of the building stock located in the study region. In addition, a significant shift in the period for maximum intensity has been observed between bedrock and surface level uniform hazard spectrum. The amplification factor observed

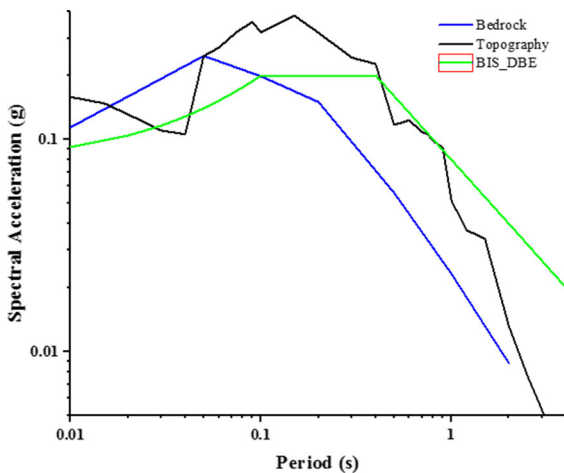


Figure 20

Comparison of the response spectra generated at the bedrock level and surface level with the design spectrum specified by Indian Seismic Code

Table 7

Spectral amplification observed for various site classes classified based on shear velocity

Shear velocity (V_s) m/s	Amplification factor
180–359	1.33 to 1.85
360–649	1.62 to 1.82
650–749	1.67 to 1.82
750–799	1.63 to 1.80
800–959	1.63 to 1.64

for the study area is classified based on the shear velocity and presented in Table 7. It is evident from Table 7 that the sites corresponding to lower shear velocity are subjected to higher amplification when compared with that of the sites with higher shear velocity. Site class B and C suffers maximum amplification whereas few regions with higher PGA values at the bedrock level have witnessed lesser amplification. The estimates made in the study are for preliminary consideration alone and site-specific studies have to be undertaken for construction of important building and infrastructures.

In seismic hazard estimation, PGA has been chosen as the standard ground motion parameter for understanding the seismic potential in different regions. The highest value in the order of 0.23–0.30 g was observed in the Bellary and Raichur districts at the surface level for 10% probability of exceedance. The predominant shear velocity estimated in this region is 180–240 ms^{-1} with few areas having a higher velocity in the range of 300–360 ms^{-1} . This region is under constant mining activity and numerous earthquakes of moderate intensity and few major ones have been witnessed in the past. This region comes under seismogenic source zone 1 (SZ1) and the majority of the earthquakes are believed to be occurring due to the excessive mining activity and tectonics of Chitradurga Boundary shear along with its associated faults. For Bengaluru region, the projected PGA value at the surface level is around 0.12–0.176 g for an estimated shear velocity in the range of 180–300 ms^{-1} implying that the region is more susceptible to seismic hazard than mentioned in the code. The site amplification studies carried out by Vipin et al. (2009) demonstrates amplification factor

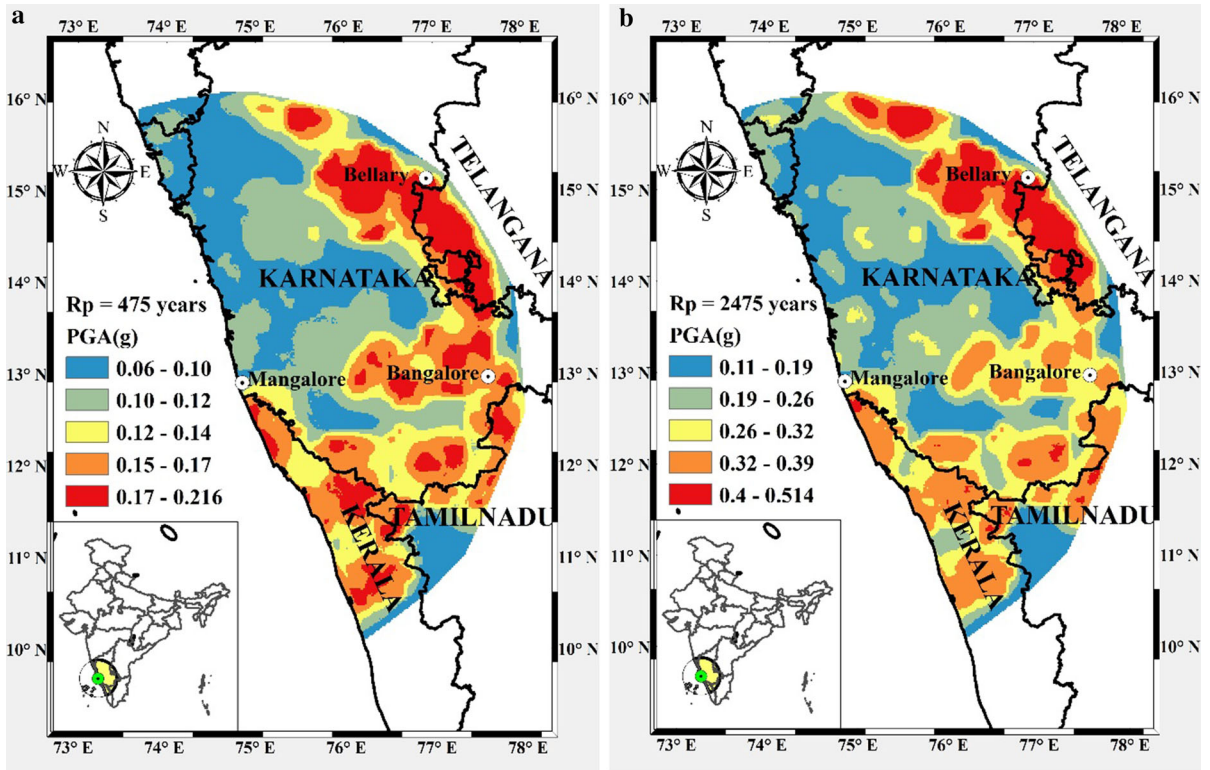


Figure 21
Contour maps representing PGA for the study area at 10% (a) and 2% (b) probability of exceedance at the surface level

in the range 1–2 for a major portion of Bengaluru with some parts experiencing higher amplification and these results are found to be in good agreement with the current research findings. The central part of Karnataka comprising of Shimoga, Chikmagalur, Chitradurga, Mysore, and Mandya districts are susceptible to low to moderate ground shaking. The mountains existing in Shimoga and Chikmagalur are mainly part of Western Ghats and not much amplification of ground motion has been observed in these districts. The Southern Coastal region covering Dakshina Kannada, a major portion of Kerala, Kodagu, and Nilgiri districts are subjected to frequent moderate ground shaking. A part of our study area encompassing Kerala is predicted to have higher seismic activity and the seismic hazard due to Bhavani and Moyar shear in association with Kaveri, Tirupur and Bhavani fault. The seismic hazard was computed for the neighboring state Goa and it was found that South Goa is more vulnerable when

compared to North Goa. Though Goa, Uttara Karnataka, Dakshina Kannada, and Kerala lie on the same coastal stretch, the seismic hazard has shown an increasing trend as one move towards South. The contour maps corresponding to 10% and 2% probability of exceedance for the study area has been plotted in Fig. 21, illustrating the variation of PGA at the surface level.

8. Conclusions

The objective of this study was to perform seismic hazard analysis for Mangalore and its surrounding area by adopting state-of-the-art classical Cornell–McGuire approach. In order to predict the seismic hazard in a probabilistic manner, all the possible seismic sources in the form of tectonic features were considered along with the up to date database of seismic activity in the region.

While attempting to understand the seismicity of the study area, it was observed that few dormant faults have undergone reactivation in the recent times and one such example is Shimoga earthquake (12th May 1975) as there were no records of past seismic activity in this region in the entire catalog duration. Also, the coastal region has witnessed very few major earthquakes and some of the shocks have originated away from the shore. The Bengaluru city is more frequently subjected to low magnitude earthquakes compared to any other region. The seismic hazard estimated for each of the mapped seismogenic source zones demonstrated that the seismic source zone 1 (SZ 1) is more vulnerable than the rest. The ongoing mining activity in Bellary and Raichur district is suspected to be the main reason for the increased seismic activity and more detailed seismic site investigation is required for this region.

The epistemic uncertainty involved in the estimation of seismic source recurrence rate and choice of GMPEs have been addressed by incorporating logic tree computation. The weights assigned for seismicity parameter estimation are based on the quantile distribution about the median values. The weights for the GMPE logic tree were based on qualitative testing, sensitivity analysis, and de-aggregation. Overall, the epistemic uncertainty is dealt with in three stages and the final outcome is a combination of all the combinations. The probabilistic seismic hazard analysis combines all potential seismic sources coupled with the possible earthquake magnitude and other factors. De-aggregation was performed to identify the most influential seismic scenario as a combination of Magnitude, Distance, and Epsilon (ϵ). The outcome of de-aggregation implied that nearby sources make a significant contribution to the seismic hazard of a specific site and also higher magnitude events have a larger spatial extent.

Sensitivity analysis has been performed for various input parameters contributing at each level of hazard calculation. Declustering, magnitude completeness, estimation of seismicity parameters, seismic source modeling and selection of GMPEs are essential steps in every hazard assessment and sensitivity analysis has been performed for each of these crucial components. Multiple methods have been adopted for each of these influential components and

the best method along with its associated end products are used for further processing the input to the hazard estimation.

The ground motion predicted at the bedrock level undergoes modification by the overlying soil layers on its way to the surface. The in situ methods are site specific but carry a certain amount of error, which cannot be quantified or remedied. In order to void this major drawback, surficial geology such as slope serving as an indirect measure of seismic characteristics was used to develop surface level seismic hazard map. With a minimal margin, the latter method can be used to estimate site-specific uniform hazard spectrum for the entire study area and also the study advocates that this method is effective and a viable option in the absence of site-specific data. The observed spectral amplification can significantly affect the low to moderate-sized buildings in the study region.

The uniform hazard spectrum developed at the bedrock level and the one generated from topography were compared with the design spectrum of IS 1893 and it was found that the majority of the study area needs an appraisal in terms of seismic zonation. Further, the seismic zoning map recommended by the Indian code is Intensity-based and not an effective standard for comparing the seismic hazard estimated using a probabilistic approach. In summary, the site-specific uniform hazard spectrum and seismic hazard maps developed from this study are believed to be of immense use for the performance-based seismic analysis and design of structures.

Acknowledgment

The authors would like to express their gratitude to Prof. Venkat Reddy, former HOD of Dept. of Civil Engineering, NITK Surathkal for his suggestions and timely advice. Indian Meteorological Department for mailing the earthquake data in time and Institute of Seismological Research for lending their resources in the successful completion of the present study. The authors would like to acknowledge the developers of CRISIS for their timely response to the clarifications sought during the study.

Publisher's Note Springer Nature remains neutral with regard to jurisdictional claims in published maps and institutional affiliations.

REFERENCES

- Aguilar-Meléndez, A., Schroeder, M. G. O., De la Puente, J., González-Rocha, S. N., Rodríguez-Lozoya, H. E., Córdova-Ceballos, A., et al. (2017). Development and validation of software CRISIS to perform probabilistic seismic hazard assessment with emphasis on the recent CRISIS2015. *Computación y Sistemas*, 21(1), 67–90.
- Aki, K. (1965). 17. Maximum likelihood estimate of b in the formula $\log N = a - bM$ and its confidence limits.
- Akkar, S., Sandikkaya, M.A. & Bommer, J.J. (2014). Empirical ground-motion models for point- and extended-source crustal earthquake scenarios in Europe and the Middle East. *Bulletin of Earthquake Engineering*, 12, 359–387. <https://doi.org/10.1007/s10518-013-9461-4>.
- Allen, T. I., & Wald, D. J. (2009). On the use of high-resolution topographic data as a proxy for seismic site conditions (VS30). *Bulletin of the Seismological Society of America*, 99(2A), 935–943.
- Amante, C., & Eakins, B.W. (2009). ETOPO1 1 Arc-minute global relief model: Procedures, data sources and analysis. NOAA Technical Memorandum NESDIS NGDC-24. National Geophysical Data Center, NOAA. <https://doi.org/10.7289/v5c8276m>. Accessed 28 Feb 2018.
- Amateur Seismic Centre, <http://www.asc-india.org/>, Pune, India. Accessed 31 Mar 2017.
- Anbazhagan, P., Vinod, J. S., & Sitharam, T. G. (2009). Probabilistic seismic hazard analysis for Bangalore. *Natural Hazards*, 48(2), 145–166.
- Ashish, Lindholm, C., Parvez, I. A., & Kühn, D. (2016). Probabilistic earthquake hazard assessment for peninsular India. *Journal of Seismology*, 20(2), 629–653. <https://doi.org/10.1007/s10950-015-9548-2>.
- Atkinson, G. M., & Boore, D. M. (2006). Earthquake ground-motion prediction equations for eastern North America. *Bulletin of the Seismological Society of America*, 96(6), 2181–2205.
- Atkinson, G. M., & Boore, D. M. (2011). Modifications to existing ground-motion prediction equations in light of new data. *Bulletin of the Seismological Society of America*, 101(3), 1121–1135.
- Balasubrahmanyam, M. N. (2006). Geology and tectonics of India An overview (No. 9).
- Bansal, B. K., & Gupta, S. (1998). A glance through the seismicity of peninsular India. *Geological Society of India*, 52(1), 67–80.
- Bazzurro, P., & Cornell, C. A. (1999). Disaggregation of seismic hazard. *Bulletin of the Seismological Society of America*, 89(2), 501–520.
- Bhatia, S. C., Kumar, M. R., & Gupta, H. K. (1999). A probabilistic seismic hazard map of India and adjoining regions. *Annals of Geophysics*, 42(6).
- Bommer, J. J., & Abrahamson, N. A. (2006). Why do modern probabilistic seismic-hazard analyses often lead to increased hazard estimates? *Bulletin of the Seismological Society of America*, 96(6), 1967–1977.
- Bommer, J. J., Douglas, J., Scherbaum, F., Cotton, F., Bungum, H., & Fäh, D. (2010). On the selection of ground-motion prediction equations for seismic hazard analysis. *Seismological Research Letters*, 81(5), 783–793.
- Bommer, J. J., & Scherbaum, F. (2008). The use and misuse of logic trees in probabilistic seismic hazard analyses. *Earthquake Spectra*, 24(4), 997–1009.
- Bommer, J. J., Stafford, P. J., Edwards, B., Dost, B., van Dedem, E., Rodríguez-Marek, A., et al. (2017). Framework for a ground-motion model for induced seismic hazard and risk analysis in the Groningen gas field, the Netherlands. *Earthquake Spectra*, 33, 481–491.
- Bott, M. H. P., & Dean, D. S. (1972). Stress systems at young continental margins. *Nature*, 235(54), 23–25.
- Campbell, K. W. (2003). Prediction of strong ground motion using the hybrid empirical method and its use in the development of ground-motion (attenuation) relations in eastern North America. *Bulletin of the Seismological Society of America*, 93(3), 1012–1033.
- CEUS Ground Motion Project Final Report, EPRI, Palo Alto, CA, Dominion Energy, Glen Allen, VA, Entergy Nuclear, Jackson, MS, and Exelon Generation Company, Kennett Square, PA: 2004. 1009684.
- Chandra, U. (1977). Earthquakes of peninsular India—A seismotectonic study. *Bulletin of the Seismological Society of America*, 67(5), 1387–1413.
- Chandrasekharan, D. (1985). Structure and evolution of the western continental margin of India deduced from gravity, seismic, geomagnetic and geochronological studies. *Physics of the Earth and Planetary Interiors*, 41(2–3), 186–198.
- Chernick, M. R. (1999). *Bootstrap methods: a practitioner's guide*. New York: Wiley Series in Probability and Statistics.
- Chopra, S., Kumar, D., Rastogi, B. K., Choudhury, P., & Yadav, R. B. S. (2013). Estimation of seismic hazard in Gujarat region, India. *Natural Hazards*, 65(2), 1157–1178.
- Cornell, C. A. (1968). Engineering seismic risk analysis. *Bulletin of the Seismological Society of America*, 58, 1583–1606.
- Cramer, C. H., & Kumar, A. (2003). 2001 Bhuj, India, earthquake engineering seismoscope recordings and Eastern North America ground-motion attenuation relations. *Bulletin of the Seismological Society of America*, 93(3), 1390–1394.
- Danciu, L., Kale, Ö., & Akkar, S. (2016). The 2014 earthquake model of the Middle East: Ground motion model and uncertainties. *Bulletin of Earthquake Engineering*, 1–37.
- Danciu, L., Monelli, D., Pagani, M., & Wiemer, S. (2010). *GEM1 hazard: review of PSHA software, gem technical Report 2010–2*. Pavia: GEM Foundation.
- Das, R., Sharma, M. L., & Wason, H. R. (2016). Probabilistic seismic hazard assessment for northeast India region. *Pure and Applied Geophysics*, 173(8), 2653–2670.
- Dasgupta, S., Narula, P. L., Acharyya, S. K., & Banerjee, J. (2000). Seismotectonic Atlas of India and its environs. Geological Survey of India.
- Desai, S. S., & Choudhury, D. (2014). Spatial variation of probabilistic seismic hazard for Mumbai and surrounding region. *Natural Hazards*, 71(3), 1873–1898.
- Edwards, B., Cauzzi, C., Danciu, L., & Fäh, D. (2016). Region-specific assessment, adjustment and weighting of ground motion prediction models: Application to the 2015 Swiss Seismic Hazard Maps. *Bulletin of the Seismological Society of America*. <https://doi.org/10.1785/0120150367>.

- ESRI. (2011). *ArcGIS desktop: release 10*. Redlands: Environmental Systems Research Institute.
- Gangrade, B. K., Prasad, A. G. V., & Sharma, R. D. (1987). Earthquakes from peninsular India: Data from the Gauribidanur seismic array (No. BARC-1347). Bhabha Atomic Research Centre.
- Gardner, J. K., & Knopoff, L. (1974). Is the sequence of earthquakes in Southern California, with aftershocks removed, Poissonian? *Bulletin of the Seismological Society of America*, 64(5), 1363–1367.
- Grünthal, G. (1998). European Macroseismic Scale 1998 (EMS-98) European Seismological Commission, sub commission on Engineering Seismology, Working Group Macroseismic Scales. Conseil de l'Europe, Cahiers du Centre Européen de Géodynamique et de Séismologie, Vol. 15, Luxembourg.
- Grünthal, G., & Wahlström, R. (2012). The European-Mediterranean earthquake catalogue (EMEC) for the last millennium. *Journal of Seismology*, 16(3), 535–570.
- Guide, R. (1997). 1.165 (1997) Identification and characterization of seismic sources and determination of safe shutdown earthquake ground motion. US Nuclear Regulatory Commission.
- Gupta, I. D. (2006). Delineation of probable seismic sources in India and neighbourhood by a comprehensive analysis of seismotectonic characteristics of the region. *Soil Dynamics and Earthquake Engineering*, 26(8), 766–790.
- Gutenberg, B., & Richter, C. F. (1944). Frequency of earthquakes in California. *Bulletin of the Seismological Society of America*, 34(4), 185–188.
- Halchuk, S., Adams, J., & Anglin, F. (2007). Revised deaggregation of seismic hazard for selected Canadian cities. In: 9th Canadian Conference on Earthquake Engineering, pp. 420–432.
- Hwang, H., & Huo, J. R. (1997). Attenuation relations of ground motion for rock and soil sites in eastern United States. *Soil Dynamics and Earthquake Engineering*, 16(6), 363–372.
- Incorporated Research Institutions for Seismology, Earthquake browser, <http://www.iris.edu/hq/>. Accessed 26 Oct 2016.
- International Seismological Centre, Online Bulletin, <http://www.isc.ac.uk>, Internat. Seismol. Cent., Thatcham, United Kingdom, 2014. Accessed on 31 Oct 2016.
- IS 1893 (Part 1). (2016). Indian standard, criteria for earthquake resistant design of structures, sixth revision, Part-I. Bureau of Indian Standards, New Delhi.
- Iyengar, R. N., Chadha, R. K., Balaji Rao, K., & Raghukanth, S. T. G. (2010). Development of probabilistic seismic hazard map of India. The National Disaster Management Authority, 86.
- Iyengar, R. N., & Ghosh, S. (2004). Microzonation of earthquake hazard in greater Delhi area. *Current Science*, 87(9), 1193–1202.
- Jaiswal, K., & Sinha, R. (2007). Probabilistic seismic hazard estimation for peninsular India. *Bulletin of the Seismological Society of America*, 97(1B), 318–330.
- Kaila, K. L., Gaur, V. K., & Narain, H. (1972). Quantitative seismicity maps of India. *Bulletin of the Seismological Society of America*, 62(5), 1119–1132.
- Raghu Kanth, S. T. G., & Iyengar, R. N. (2007). Estimation of seismic spectral acceleration in peninsular India. *Journal of Earth System Science*, 116(3), 199–214. <https://doi.org/10.1007/s12040-007-0020-8>.
- Kayal, J. R. (2008). *Microearthquake seismology and seismotectonic of South Asia*. New York: Springer Science & Business Media.
- Khattri, K. N., Rogers, A. M., Perkins, D. M., & Algermissen, S. T. (1984). A seismic hazard map of India and adjacent areas. *Tectonophysics*, 108(1–2), 93111–108134.
- Kijko, A., & Smit, A. (2012). Extension of the Aki-Utsu b-value estimator for incomplete catalogues. *Bulletin of the Seismological Society of America*, 102(3), 1283–1287.
- Kolathayar, S., & Sitharam, T. G. (2012). Characterization of regional seismic source zones in and around India. *Seismological Research Letters*, 83(1), 77–85.
- Kolathayar, S., Sitharam, T. G., & Vipin, K. S. (2012). Spatial variation of seismicity parameters across India and adjoining areas. *Natural Hazards*, 60, 1365. <https://doi.org/10.1007/s11069-011-9898-1>.
- Maiti, S. K., Nath, S. K., Adhikari, M. D., Srivastava, N., Sengupta, P., & Gupta, A. K. (2017). Probabilistic seismic hazard model of West Bengal. *India. Journal of Earthquake Engineering*, 21(7), 1113–1157.
- Martin, S., & Szeliga, W. (2010). A catalog of felt intensity data for 570 earthquakes in India from 1636 to 2009. *Bulletin of the Seismological Society of America*, 100(2), 562–569.
- Milne, J. (1911). A catalogue of destructive earthquakes: AD 7 to AD 1899. The Association.
- Musson, R. M., Grünthal, G., & Stucchi, M. (2010). The comparison of macroseismic intensity scales. *Journal of Seismology*, 14(2), 413–428.
- Nath, S. K., & Thingbaijam, K. K. S. (2012). Probabilistic seismic hazard assessment of India. *Seismological Research Letters*, 83(1), 135–149.
- National Earthquake Information Center 2003 USA PDE reportings <http://neic.usgs.gov/neis/epic/>. Accessed on 28 Nov 2016.
- Oldham, T. (1883). A Catalogue of Indian Earthquakes from the earliest time to the end of AD 1869, Memoirs of the Geological Survey of India 19 Part 3.
- Pezeshk, S., Zandieh, A., & Tavakoli, B. (2011). Hybrid empirical ground-motion prediction equations for eastern North America using NGA models and updated seismological parameters. *Bulletin of the Seismological Society of America*, 101(4), 1859–1870.
- Radhakrishna, B. P. (1993). Neogene uplift and geomorphic rejuvenation of the Indian Peninsula. *Current Science*, 787–793.
- Ganesh Raj, K., & Nijagunappa, R. (2004). Major lineaments of Karnataka state and their relation to seismicity: A remote sensing based analysis. *Journal-Geological Society of India*, 63(4), 430–439.
- Raj, K. G., Paul, M. A., Hegde, V. S., & Nijagunappa, R. (2001). Lineaments and seismicity of Kerala—A remote sensing based analysis. *Journal of the Indian Society of Remote Sensing*, 29(4), 203–211.
- Rajendran, C. P., John, B., Sreekumari, K., & Rajendran, K. (2009). Reassessing the earthquake hazard in Kerala based on the historical and current seismicity. *Journal of the Geological Society of India*, 73(6), 785–802.
- Rajendran, C. P., & Rajendran, K. (2002). Historical constraints on previous seismic activity and morphologic changes near the source zone of the 1819 Rann of Kachchh earthquake: further light on the penultimate event. *Seismological Research Letters*, 73(4), 470–479.
- Rao, B. R. (1992). Seismicity and geodynamics of the low-to high-grade transition zone of peninsular India. *Tectonophysics*, 201(1–2), 175–185.

- Rao, B. R., & Rao, P. S. (1984). Historical seismicity of peninsular India. *Bulletin of the Seismological Society of America*, 74(6), 2519–2533.
- Rastogi, B. K. (2016). Seismicity of Indian stable continental region. *Journal of Earthquake Engineering*, 3, 57–93.
- Rastogi, B. K., Chadha, R. K., & Sarma, C. S. P. (1995). Investigations of June 7, 1988 earthquake of magnitude 4.5 near Idukki Dam in southern India. *Pure and Applied Geophysics*, 145(1), 109–122.
- Reddy, P. R., & Rao, V. V. (2000). Structure and tectonics of the Indian peninsular shield—Evidences from seismic velocities. *Current Science*, 899–906.
- Rout, M. M., Das, J., & Kamal (2018). Probabilistic seismic hazard for Himalayan region using kernel estimation method (zone-free method). *Natural Hazards*, 93(2), 967–985.
- Seeber, L., Armbruster, J. G. & Jacob, K. H. (1999) Probabilistic assessment of earthquake hazard for the State of Maharashtra, India. The Government of Maharashtra Earthquake Rehabilitation Cell, Mumbai, p. 60.
- Singh, S. K., Bansal, B. K., Bhattacharya, S. N., Pacheco, J. F., Dattatrayam, R. S., Ordaz, M., et al. (2003). Estimation of ground motion for Bhuj (26 January 2001; Mw 7.6) and for future earthquakes in India. *Bulletin of the Seismological Society of America*, 93(1), 353–370.
- Sitharam, T. G., & Anbazhagan, P. (2007). Seismic hazard analysis for the Bangalore region. *Natural Hazards*, 40(2), 261–278.
- Sitharam, T. G., James, N., Vipin, K. S., & Raj, K. G. (2012). A study on seismicity and seismic hazard for Karnataka State. *Journal of Earth System Science*, 121, 1–16.
- Sitharam, T. G., & Kolathayar, S. (2013). Seismic hazard analysis of India using areal sources. *Journal of Asian Earth Sciences*, 62, 647–653.
- Sitharam, T. G., Kolathayar, S., & James, N. (2015). Probabilistic assessment of surface level seismic hazard in India using topographic gradient as a proxy for site condition. *Geoscience Frontiers*, 6(6), 847–859.
- Srivastava, H. N., & Ramachandran, K. (1985). New catalogue of earthquakes for peninsular India during 1839–1900. *Mausam*, 36(3), 351–358.
- Stepp, J. C. (1973). Analysis of completeness of the earthquake sample in the Puget Sound area. Seismic zoning edited by ST Harding NOAA Tech. Report ERL.
- Subrahmanya, K. R. (1996). Active intraplate deformation in south India. *Tectonophysics*, 262(1–4), 231–241.
- Sykes, L. R. (1970). Seismicity of the Indian Ocean and a possible nascent island arc between Ceylon and Australia. *Journal of Geophysical Research*, 75(26), 5041–5055.
- Toro, G. R. (2002). Modification of the Toro et al. (1997) attenuation equations for large magnitudes and short distances. Risk Engineering Technical Report.
- Toro, G. R., Abrahamson, N. A., & Schneider, J. F. (1997). Model of strong ground motions from earthquakes in central and eastern North America: best estimates and uncertainties. *Seismological Research Letters*, 68(1), 41–57.
- Uhrhammer, R. (1986). Characteristics of Northern and Central California Seismicity. *Earthquake Notes*, 57(1), 21.
- Valdiya, K. S. (1989). Neotectonic implication of collision of Indian and Asian plates. *Indian Journal of Geology*, 61, 1–13.
- Valdiya, K. S. (2013). Recent tectonic movements in the Kaveri catchment, southern India. *Journal of the Indian Institute of Science*, 77(3), 267.
- Verma, M., & Bansal, B. K. (2013). Seismic hazard assessment and mitigation in India: an overview. *International Journal of Earth Sciences*, 102(5), 1203–1218.
- Vipin, K. S., Anbazhagan, P., & Sitharam, T. G. (2009). Estimation of peak ground acceleration and spectral acceleration for South India with local site effects probabilistic approach. *Natural Hazards and Earth System Sciences*, 9(3), 865.
- Vipin, K. S., & Sitharam, T. G. (2013). Delineation of seismic source zones based on seismicity parameters and probabilistic evaluation of seismic hazard using logic tree approach. *Journal of Earth System Science*, 122(3), 661–676.
- Wiemer, S. (2001). A software package to analyze seismicity: ZMAP. *Seismological Research Letters*, 72(3), 373–382.
- Woessner, J., & Wiemer, S. (2005). Assessing the quality of earthquake catalogues: Estimating the magnitude of completeness and its uncertainty. *Bulletin of the Seismological Society of America*, 95(2), 684–698.
- Indian Meteorological Department (IMD), www.imd.gov.in/, New Delhi, India (Through Personal communication).

(Received November 22, 2017, revised December 12, 2018, accepted January 16, 2019)